

AD-A105 126

VARIAN ASSOCIATES INC PALO ALTO CA
DISPENSER CATHODE PHYSICS.(U)
JUL 81 M C GREEN

F/G 9/1

F30602-79-C-0220

UNCLASSIFIED

RADC-TR-81-211

NL

1 1
40 A
1-10-81

1 1
40 A
1-10-81

END
DATE
FILMED
0 81
DTIC

AD A105126

RADC-TR-81-211
Final Technical Report
July 1981



LEVEL



DISPENSER CATHODE PHYSICS

Varian Associates, Inc.

Michael C. Green

1-800
821770

APPROVED FOR PUBLIC RELEASE; DISTRIBUTION UNLIMITED

DTIC
ELECTE
OCT 6 1981
S D
B

FILE COPY


ROME AIR DEVELOPMENT CENTER
Air Force Systems Command
Griffiss Air Force Base, New York 13441

81 10 5 177

This report has been reviewed by the RADC Public Affairs Office (PAO) and is releasable to the National Technical Information Service (NTIS). At NTIS it will be releasable to the general public, including foreign nations.

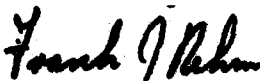
RADC-78-81-211 has been reviewed and is approved for publication.

APPROVED:



ALBERT F. MORRELL
Project Engineer

APPROVED:



FRANK J. REHM
Technical Director
Surveillance Division

FOR THE COMMANDER:



JOHN P. HUSS
Acting Chief, Plans Office

If your address has changed or if you wish to be removed from the RADC mailing list, or if the addressee is no longer employed by your organization, please notify RADC (OCTP) Griffiss AFB NY 13441. This will assist us in maintaining a current mailing list.

Do not return this copy. Retain or destroy.

MISSION **of** **Rome Air Development Center**

RADC plans and executes research, development, test and selected acquisition programs in support of Command, Control Communications and Intelligence (C³I) activities. Technical and engineering support within areas of technical competence is provided to ESD Program Offices (POs) and other ESD elements. The principal technical mission areas are communications, electromagnetic guidance and control, surveillance of ground and aerospace objects, intelligence data collection and handling, information system technology, ionospheric propagation, solid state sciences, microwave physics and electronic reliability, maintainability and compatibility.

UNCLASSIFIED

SECURITY CLASSIFICATION OF THIS PAGE (When Data Entered)

REPORT DOCUMENTATION PAGE		READ INSTRUCTIONS BEFORE COMPLETING FORM
1. REPORT NUMBER RADC-TR-81-211	2. GOVT ACCESSION NO. AD-105 126	3. RECIPIENT'S CATALOG NUMBER
4. TITLE (and Subtitle) DISPENSER CATHODE PHYSICS.	5. TYPE OF REPORT & PERIOD COVERED Final Technical Report. 1 Aug 79 - 1 Nov 80	6. PERFORMING ORG. REPORT NUMBER N/A
7. AUTHOR(s) Michael C. Green	8. CONTRACT OR GRANT NUMBER(s) F30602-79-C-0220	
9. PERFORMING ORGANIZATION NAME AND ADDRESS Varian Associates, Inc. 611 Hansen Way Palo Alto CA 94304	10. PROGRAM ELEMENT, PROJECT, TASK AREA & WORK UNIT NUMBERS 62702F 45061260	
11. CONTROLLING OFFICE NAME AND ADDRESS Rome Air Development Center (OCTP) Griffiss AFB NY 13441	12. REPORT DATE Jul 1981	13. NUMBER OF PAGES 92
14. MONITORING AGENCY NAME & ADDRESS (if different from Controlling Office) Same	15. SECURITY CLASS. (of this report) UNCLASSIFIED	15a. DECLASSIFICATION/DOWNGRADING SCHEDULE N/A
16. DISTRIBUTION STATEMENT (of this Report) Approved for public release, distribution unlimited.		
17. DISTRIBUTION STATEMENT (of the abstract entered in Block 20, if different from Report) Same		
18. SUPPLEMENTARY NOTES RADC Project Engineer: Albert F. Morreall (OCTP)		
19. KEY WORDS (Continue on reverse side if necessary and identify by block number) XPS (x-ray photoelectron Spectroscopy) Auger Spectroscopy		
20. ABSTRACT (Continue on reverse side if necessary and identify by block number) The structure and composition of the emissive layers of activated and stabilized B-type and M-type cathode surfaces at operating temperature were investigated using X-ray photoelectron spectroscopy and high spatial resolution Auger Spectroscopy. The results indicate that the activating layer consists of a monolayer or submonolayer film of barium and oxygen of stoichiometry close to Ba ₁ O ₁ . The emissive layer was found to be vertically ordered, with barium concentrated in the first monolayer above		

DD FORM 14/3 EDITION OF 1 NOV 65 IS OBSOLETE

UNCLASSIFIED

SECURITY CLASSIFICATION OF THIS PAGE (When Data Entered)

UNCLASSIFIED

SECURITY CLASSIFICATION OF THIS PAGE(When Data Entered)

oxygen. The primary difference observed between the B-type and M-type surfaces was increased coverage of the underlying metal by the barium/oxygen layer in the M-type case. The spectra of the emissive layer, although quite different from those of "bulk" barium oxide, were consistent with a barium-oxygen bonding interaction.

A theoretical model of the bonding of barium and oxygen to each other and to the underlying metal matrix surface was proposed, consistent with the above experimental data and with the published results of other workers in the field. A calculation of the lattice stabilization energy in bulk ionic BaO indicated that the bonding in the emissive layer must be predominantly covalent. A covalent bonding scheme for the barium-oxygen linkage and also for the oxygen-metal surface link in the Ba-O-metal sandwich of the emissive layer was constructed. A classification system in terms of metal surface d-orbitals was applied to the metals normally employed on dispenser cathode surfaces and correlated with their emission enhancement capability. The mechanism of emission enhancement (or degradation) was accounted for in terms of O-donor bonding to vacant metal surface d-orbitals. This model was extended to account for emission differences between differing crystal planes of the same metal and also for the emission enhancing action of tungsten-iridium and tungsten-osmium alloys. A distinction was drawn between the chemical state of the emissive monolayer and that of barium oxide even in thin layers.

In Appendix A, a new user-oriented method of plotting cathode emission test data in the form of Miram-plots of normalized current density against temperature is described. Examples are given of the manner in which such plots clearly delineate changes in cathode performance capability with time and specific cathode failure modes. The cathode physics of a novel failure mode of a high current density cathode involving saturation of pore center emission is described.

UNCLASSIFIED

SECURITY CLASSIFICATION OF THIS PAGE(When Data Entered)

TABLE OF CONTENTS

<u>Section</u>	<u>Page</u>
1. INTRODUCTION	1
2. TASK DEFINITION	2
3. HISTORICAL REVIEW	3
4. EXPERIMENTAL APPROACH	8
5. RESULTS AND DISCUSSION	17
5.1 Comparison of M-type and B-type Surfaces and Measurement of Emissive Layer Thickness and Composition	17
5.2 Other Changes During Activation	20
5.3 High Resolution Measurements of Emissive Layer Thickness and Composition	22
5.4 X-ray Photoelectron Studies of Cathode Surfaces	33
6. A PROPOSED NEW MODEL FOR THE EMISSIVE LAYER STRUCTURE AND BONDING IN DISPENSER CATHODES AND FOR THE EMISSION ENHANCEMENT MECHANISM IN "M-TYPE" AND RELATED HIGH CURRENT DENSITY CATHODES	42
6.1 Theoretical Model	45
7. SUMMARY AND CONCLUSIONS	69
8. REFERENCES	71
Appendix A - An Electron Optical Investigation of Pore Emission Phenomena in High Current Density Dispenser Cathodes	

Accession For		
NTIS	GRA&I	<input checked="" type="checkbox"/>
DTIC TAB		<input type="checkbox"/>
Unannounced		<input type="checkbox"/>
Justification		
By		
Distribution/		
Availability Codes		
Dist	Avail and/or	Special
A		

LIST OF ILLUSTRATIONS

<u>Figure</u>		<u>Page</u>
1.	Scale of Cathode Surface Features	9
2.	Cross Section Through Cathode Surface Showing Changes with Life	10
3.	Purpose - Built Surface Analysis System for Cathode Physics Studies	11
4.	Varian Scanning Auger Microprobe Electron Gun Performance	14
5.	Total Secondaries Image of Dispenser Cathode Using Varian Sam Showing Resolved Pores and Grain Tops (2K X)	15
6.	Single Element Auger Linescans Across Interface Between B-type and M-type Cathode Surfaces	19
7.	Loss of Oxygen Due to Stimulated Desorption Damage with Stationary Beam	23
8.	Tungsten and Osmium High Energy Auger Lines Showing Separation and Signal-to-Noise	26
9.	Auger Spectrum of Tungsten Sample High Energy Region with 3 keV Incident Beam	27
10.	Full Width Auger Spectrum of Activated B-type Surface	29
11.	Auger Spectrum of Activated M-type Surface	30
12.	Plot of O/W and Ba/W Auger Signal Ratios for Interpore Regions of Activated B-type and M-type Surfaces	31
13.	Variation in Equivalent Escape Depth with Exit Angle for Photoelectrons Originating Below the First Monolayer	35
14.	X-ray Photoelectron Spectrum of Clean Osmium Reference Surface	36
15.	X-ray Photoelectron Spectrum of M-type Cathode Surface Prior to Activation	37
16.	X-ray Photoelectron Spectrum of Activated M-type Cathode Surface	38

LIST OF ILLUSTRATIONS

17.	Variation in Barium and Oxygen Photoelectron Count-Rate Ratio at 45° and 10° Surface Exit Angle for Activated M-type Surface at 1000°C_B	41
18.	The Barium Oxide Crystal Lattice Structure	47
19.	Covalent Bonding in "Molecular" BaO	51
20.	sp^2 Hybridization of Oxygen Showing Orbital Occupancy	54
21.	Average Emission Enhancement Ratio vs Average Bare Work Function	58
22.	Covalent Bonding to Metal Surface d-Orbitals	61

1. INTRODUCTION

The impregnated dispenser cathode is a rugged device that has found many applications in the vacuum tube industry; it is now the industry standard cathode for high power microwave tubes. However, recent advances in tube performance capability and power output, particularly in the millimeter wave region, have generated requirements for current density/cathode life combinations which present-day cathodes cannot reliably meet.

This program was undertaken with the objective of achieving an improved theoretical understanding of the basic processes controlling electron emission from the types of dispenser cathodes commonly used in microwave tubes. The physics of electron emission from dispenser cathodes is still an area of intense debate among workers in the field. Increased knowledge of the microstructure of the emissive layer and its relation to thermionic emission capability should provide useful guidelines for the design of future improved cathodes without recourse to costly and time-consuming empirical engineering.

Investigations were conducted in two main areas: (1) measurements of the composition, thickness and internal structure of the emissive surface layer of cathodes at operating temperature under ultra high-vacuum conditions utilizing a purpose built surface analysis system, and (2) an electron optical study of the factors, such as patch fields and pore size, which limit the attainable cathode current density in realistic cathodes.

2. TASK DEFINITION

As defined in the statement of work for this contract, the requirements of this program were to carry out a three-phase study.

The initial requirement was to search the literature for prior work on the physics of electron emission from dispenser cathodes, then to segregate the various hypotheses put forward regarding the mechanism of this process and select potentially workable hypotheses applicable to metal matrix cathodes. In phase two, the task was to study working cathodes by means of surface analysis. The analyses were to be directed towards the emissive regions of (a) standard tungsten matrix barium-calcium aluminate impregnated cathodes, and (b) high current density derivatives of the basic cathode where platinum group metals, such as osmium or iridium, have been employed as emission-enhancing additives. During phase three, a workable hypothesis was to be developed consistent with the above experimental results and with the results of other workers in the field capable of explaining the emission mechanisms in metal matrix cathodes.

3. HISTORICAL REVIEW

Since the 1920's, much work has been published on the theory of operation of electron emitters. The early work was, of course, primarily concerned with the oxide cathode; but in more recent years, the demand for higher current density capability has promoted the introduction of the dispenser cathode into many microwave tube applications. These cathodes are now the industry norm.

Further enhanced-emission capabilities have been demonstrated more recently by a modification of the basic dispenser cathode, the "M-type" cathode, in which a layer of 80/20 osmium/ruthenium is sputter coated onto the cathode surface. This cathode shows a better than twofold increase in emission density associated with an order of magnitude reduction in evaporation rate when compared with the basic barium-calcium aluminate tungsten dispenser cathode. More recently still, alloy matrix cathodes such as the iridium-tungsten matrix have shown promise of additional improvement in attainable emission density and life.

It is not the purpose of this review to present a survey of the very voluminous literature on cathode research, but merely to briefly summarize the current position of the various schools of thought regarding the basic mechanisms of emission. An extremely comprehensive literature survey of the entire field covering the time period 1947 - 1960 (i.e., all the basic work on the dispenser cathode prior to the development of the M-type cathode) was carried out by Armour Research Foundation under the auspices of RADC¹. This contains a full compilation of the literature covering cathodes, electron emission processes and related areas up to early 1960.

The impregnated cathode was first reported by Levi² in 1953 and was a natural derivative of the so-called L cathode developed earlier by Lemmens and co-workers³. The L cathode was capable of CW current densities at least an order of magnitude higher than an oxide cathode, although at the rather high temperature of 1250°C, with a life of some 2000 hours. Originally the impregnated cathode, containing a barium oxide/alumina melt, gave roughly a factor of five lower current density than the L cathode; however, Levi⁴

found that by adding calcium oxide to the impregnant, the current density capability could be made comparable to that of the L cathode. This embodiment constituted the Philips B-type cathode with an impregnant mix of $5 \text{ BaO}-3 \text{ CaO}-2 \text{ Al}_2\text{O}_3$.

In the 1960's, Zalm⁵ reported a further improvement in emission density capability achieved by sputter coating the emitting surface of the impregnated cathode with a thin (4000 Å) layer of osmium. In its final form the "M-type" cathode was coated with a layer of 80/20 osmium/ruthenium.

The emitter of the typical impregnated cathode today is essentially unchanged from Levi's development. It consists of an indirectly heated porous tungsten matrix fabricated from 4-5 μ average grain size powder, which is isostatically pressed and sintered to give an overall porosity of around 20% with good pore interconnectivity. The tungsten pellet is impregnated with a melt of mixed calcined $\text{BaO}-\text{CaO}-\text{Al}_2\text{O}_3$ drawn into the pores by capillary action in an atmosphere of dry hydrogen. After activation in vacuum (10^{-7} torr or better) at $1190^\circ\text{C}_\text{B}$, the cathode is capable of 2 A/cm^2 at $1050^\circ\text{C}_\text{B}$, and ongoing life tests in excess of 48,000 hours exist at this current density.

Despite the apparent simplicity of the construction of dispenser cathodes, the chemical reactions occurring within them and the detailed structure of the surface emitting layer are complex. Furthermore, due to the extreme sensitivity of the emitting surface to contamination and also the small scale spatial inhomogeneity of the emitting region, direct study of the emissive layer presents formidable experimental difficulties.

Much work has been performed over the years, therefore, on model systems; and while the basic constituents of the emitting region of the cathode are known to be barium and oxygen two different (and opposed) schools of thought have arisen, each supported by considerable experimental evidence. One hypothesis supports a thin layer type of emitter comprising a monolayer or less of metallic barium on a partially oxygenated tungsten surface, and the other a bulk type emitter where the active sites are relatively thick layers or even microcrystallites of barium oxide activated

by excess barium in a manner analogous to the older oxide coated cathode. This difference is nontrivial, as the mechanism for emission enhancement would be completely different in the two cases.

Models presented by Rittner, Rutledge and Ahlert^{6,7,8} in a series of papers in the late fifties have cited evidence in support of a barium monolayer type emitter with the presence of oxygen inferred to account for the low barium evaporation rate from the cathode surface. Further work by Springer and T.W. Haas⁹ and by Foreman^{10,11} using Auger spectroscopy on both model surfaces and on actual cathodes has indicated an emitting surface consisting of a monolayer or less of barium over oxygen upon tungsten.

Conversely Druzhinin¹², using emission microscopy, has published evidence for the formation of barium oxide crystallites at the active sites, and Beck and Ahmed¹³ have presented results from scanning electron microscopy and Auger spectroscopy indicating the presence of thick barium oxide layers on the cathode surface. G.A. Haas¹⁴ has modeled the activating effect of iridium on barium oxide using thick epitaxial BaO layers on Ir 100 single crystal surfaces.

As recently as the last TriServices Cathode Workshop, held at RADC in April 1980, papers were presented adducing evidence for both the thick layer^{15,16} and the thin layer¹⁷ hypotheses. Particularly in the case of the thin layer hypothesis, there is much disagreement over the composition, chemical state and surface binding of the monolayer film.

Even less well understood than the emission mechanism of standard tungsten dispenser cathodes is the mode by which osmium, iridium and other platinum group metals (but not platinum itself) enhance emission in the M-type cathode and its derivatives. Current work at Varian Associates, at EMI-Varian¹⁸, and work on polycrystalline iridium surfaces by R.E. Thomas at NRL¹⁹ indicates that the majority of the early work on M-type cathodes and particularly that relating to their complex end-of-life behavior has led to erroneous conclusions.

Such studies have led to the development at Varian of the tungsten-iridium matrix cathode having emission properties comparable or superior to the M-type cathode combined with far greater tolerance of adverse operating environments and increased life. These developments are continuing, for the first time not wholly on an empirical basis but with an increasing understanding of the actual engineering parameters involved.

Nonetheless, despite the great number of excellent studies reported and conclusions published, there are still many contradictions and grey areas in the explanations of the operating mechanism of the types of cathode which are now the industry standard in microwave tubes. Vigorous and even acrimonious dispute has occurred between proponents of different hypotheses. Partly this is possible because of the extreme difficulty of making meaningful measurements on the fragile emissive layer, which is in continuous dynamic equilibrium between supply from the matrix and loss via sputtering and evaporation to the surroundings. This equilibrium is only possible at high temperatures and under ultrahigh vacuum conditions.

Only recently has the state of the art in surface analysis equipment reached a level where achievable resolution and sensitivity gives the capability of making unambiguous and quantitative measurements on cathodes at the atomic level, localized to the first few monolayers or even the first monolayer of the surface. This, coupled with developments in millimeter wave tube technology with its attendant demands for increased beam current density, has led to a resurgence of interest in cathode physics.

Many questions remain unanswered. Important amongst these are the nature of the role played by oxygen in the emitting layer; its source, chemical state and the amount present are all areas of debate. Similarly, the chemical state of the barium is an open question: Is it metallic, present as an oxide, or in some intermediate form? What is the degree of surface coverage, and how does this relate to localized emission capability? Equally vital is understanding the interaction of the emissive layer with the underlying metal surface. What is the nature of the strong bonding between the barium/oxygen and the metal? Especially relevant to high current density cathodes, what is the mechanism by which osmium, iridium and

certain other platinum group metals produce such a dramatic increase in emissive capability in the M-type cathode and its derivatives?

4. EXPERIMENTAL APPROACH

Dispenser cathodes present peculiar problems for analysis, not merely because of the required operating conditions ($\sim 1050^{\circ}\text{C}_B$ and ultra high vacuum), but because of the small physical size of the surface features (Figure 1). Typically, the grains of the porous metal matrix average 4-5 microns in diameter. The pores between the grains average <3 microns equivalent diameter with a mean interpore spacing of 6 microns. These are only the gross features of the emissive surface, and large variations in emission density are known to occur on an even smaller spatial scale.

Any meaningful chemical analysis of the emissive region, therefore, must not only be confined to the extreme surface, but must be capable of distinguishing laterally between such features as pores and grains. Otherwise, the large amounts of barium and oxygen containing impregnant material present in the pores will completely dominate the signals from the grain tops which constitute 80% of the emissive surface but which have only a very thin covering of activator.

A further problem arises from the lengthy time scale over which changes in dispenser cathodes occur. Although initial activation requires a matter of hours only, major changes take place (see Figure 2) over typically the first 1000 hours of life at 1050°C_B (less than 2% of the potential life of the device at that temperature). Measurements made during this stabilization period, although obviously informative, cannot be regarded as typical of the surface during the vast majority of its life. Since transfer from test diodes, etc., involves breaking the vacuum, it is desirable to be able to run the test cathodes within the analysis system itself for hundreds or even thousands of hours.

With these considerations in mind the Palo Alto Microwave Tube Division has set up a dedicated surface analysis facility designed specifically for cathode physics studies (Figure 3). The equipment is all contained within a bakeable UHV all-metal system using sorption, VacIon^R and titanium sublimation pumping and capable of attaining base pressures in the 10^{-11} torr region.

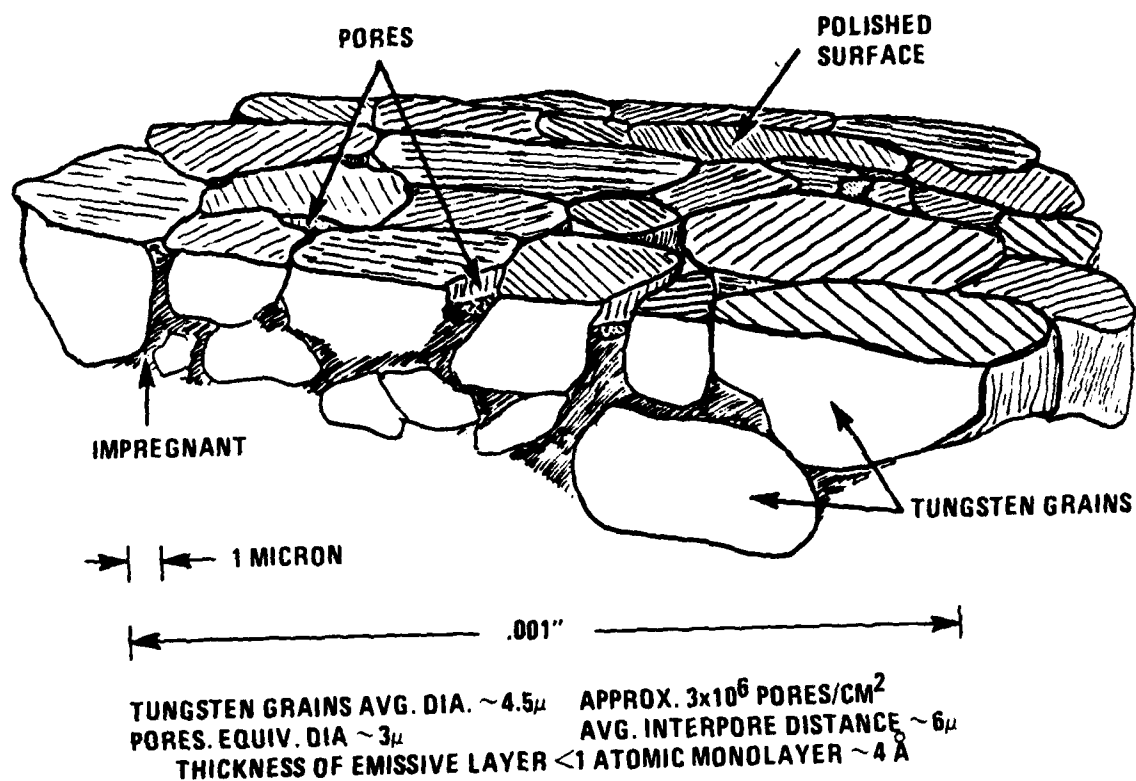


FIGURE 1. SCALE OF CATHODE SURFACE FEATURES

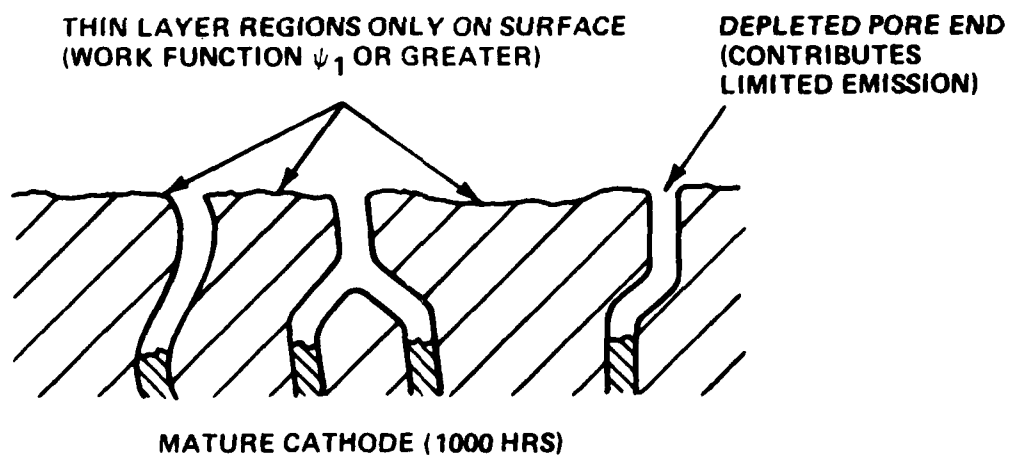
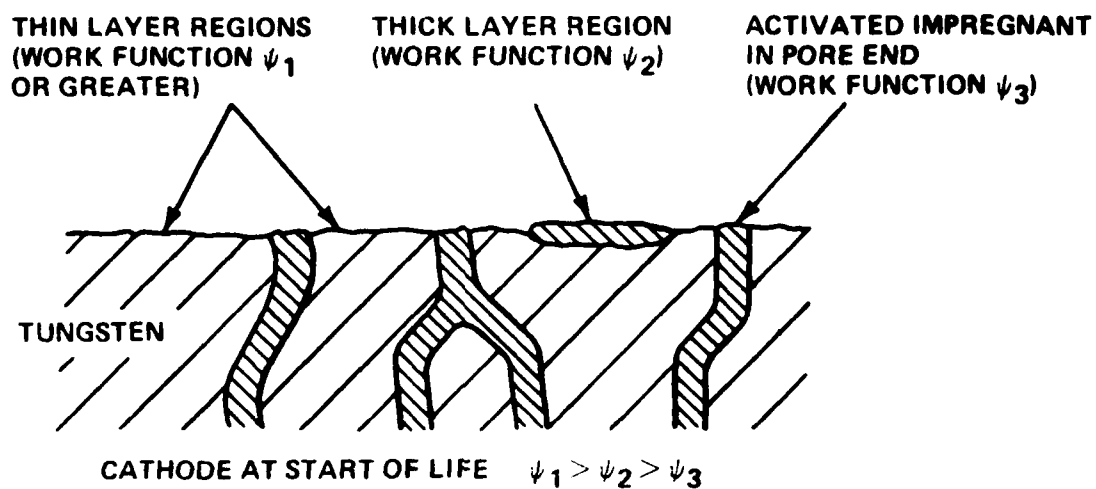


FIGURE 2. CROSS SECTION THROUGH CATHODE SURFACE SHOWING CHANGES WITH LIFE

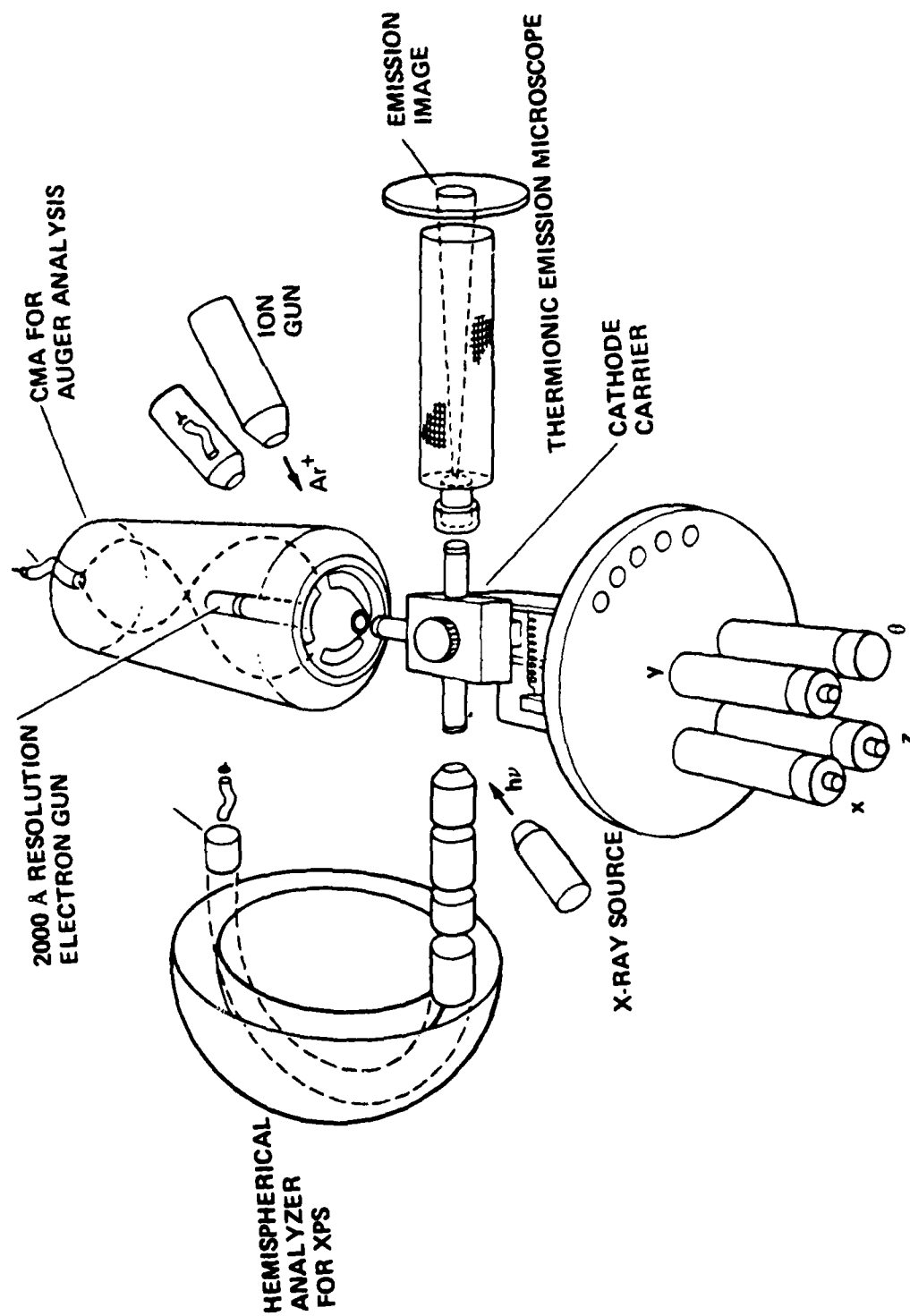


FIGURE 3. PURPOSE-BUILT SURFACE ANALYSIS SYSTEM FOR CATHODE PHYSICS STUDIES

Cathodes under test are mounted on an electrically isolated carrousel attached to a high precision manipulator capable of rotation and of x, y and z motion with one micron positioning accuracy. They can be moved between several analysis stations, the first of which is a thermionic emission microscope (THEM).

The THEM uses an electrostatic lens to image an 0.006" diameter region of the cathode surface onto a phosphor screen with a magnification of 200X. A further stage of optical magnification permits the resolution of emission features $\sim 2000 \text{ \AA}$ in size. The current densities in small microelements of the image can be obtained by measuring their brightness in the magnified image, a method giving greater spatial resolution than a Faraday cup collector in the microscope drift space. The modulator electrode of the microscope which is adjacent to the cathode is made from a flat, polished molybdenum disc. By applying appropriate potentials this can be used as a planar anode for emission testing.

The next analysis station (moving counterclockwise) is occupied by the heart of the system, a scanning Auger Microprobe (SAM). Here a rasterable high resolution electron gun is mounted coaxially with a double pass cylindrical mirror analyzer (CMA). The CMA collects electrons leaving the sample at an angle of approximately 43.5° to the normal over a full circle. This solid of resolution is equivalent to $\sim 7\%$ of 2π steradians at the input.

The key to the performance of the SAM is the electron gun. Since Auger electrons comprise only a very small proportion ($\sim 10^{-3}$) of all secondaries, a relatively high beam current must be deposited in the sample in order to get adequate signal. Scanning electron microscopes which collect "total secondaries" achieve very high spatial resolution but with beam currents of the order of 10^{-10} amperes or less. For Auger work, currents in the 10^{-6} ampere region are desirable. Most previous systems have therefore used beam spot diameters of several microns or even tens of microns to get sufficient deposited current.

For cathode work, submicron spatial resolution is vital; and the Varian SAM electron gun, which uses an extremely high brightness electron source, provides this capability while still providing adequate beam current to the sample. The gun performance is shown in Figure 4. The resolution limit is approximately 2000 Å and the gun will provide submicron resolution with a beam current approximately 10^{-6} amperes. The high brightness emitter within the gun employs an in-house manufactured state-of-the-art dispenser cathode. This gives current densities comparable to the LaB_6 source more often used, but at much lower temperature and with much greater uniformity of emission. This latter feature gives a considerable improvement in resolution and thermal stability of the gun.

Simple adjustment of the gun electrode voltages allows a rapid trade-off of resolution against beam current. Thus, the sample may be imaged in "total secondaries" mode at high resolution (Figure 5) and then Auger analysis carried out with higher beam current and with resolution just sufficient to distinguish the features of interest. The gun control electronics permit Auger point analysis, Auger line scan analysis and Auger elemental mapping. An argon ion gun mounted confocally with the electron gun enables depth profiling to be carried out.

The third analysis station is fitted with an X-ray photoelectron spectrometer (XPS) system. A twin anode X-ray source illuminates the sample surface with either Al K α or Mg K α X-rays, and the resultant photoelectrons are collected by an electron lens system and collimated into a hemispherical electrostatic energy analyzer. The hemispherical analyzer, in combination with pre-retardation grids, gives very high energy resolution capability. This permits the measurement of small "chemical shifts" in the photoelectron energies and hence the determination of the exact state of chemical combination of the sample elements.

The hemispherical analyzer has the further virtue that its acceptance angle for electrons is very narrow in the radial plane. By rotating the sample in this plane angularly, resolved photoelectron emission measurements

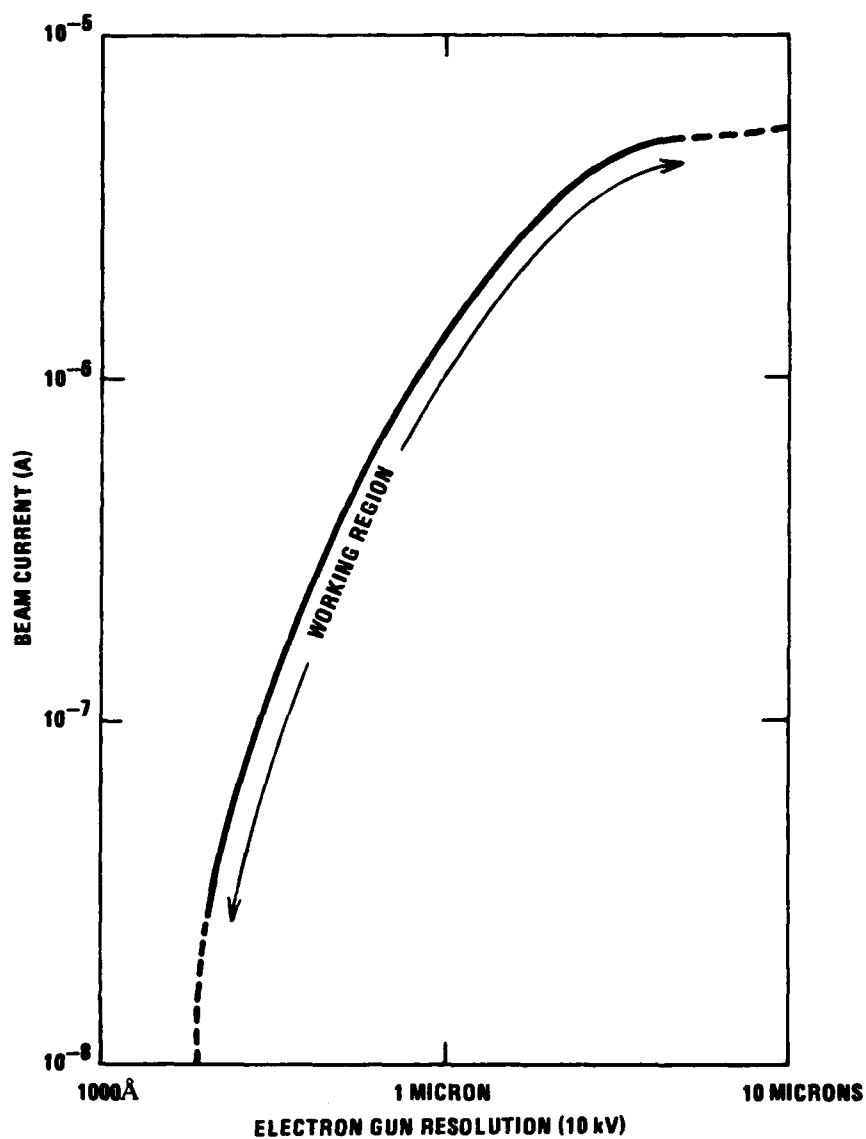


FIGURE 4. VARIAN SCANNING AUGER MICROPROBE
ELECTRON GUN PERFORMANCE



**FIGURE 5. TOTAL SECONDARIES IMAGE OF DISPENSER CATHODE USING
VARIAN SAM SHOWING RESOLVED PORES AND GRAIN TOPS (2K X)**

may be made and much additional information about the sample surface structure obtained; for example, the vertical ordering of the first few atomic layers.

5. RESULTS AND DISCUSSION

5.1 COMPARISON OF M-TYPE AND B-TYPE SURFACES AND MEASUREMENT OF EMISSIVE LAYER THICKNESS AND COMPOSITION

For initial experiments a standard dispenser with 4:1:1 mole ratio impregnant cathode was manufactured, "M-coated" with a 4000 Å sputtered layer of 80% osmium 20% ruthenium, and then the sputtered film was removed mechanically from one half of the cathode surface. The cathode was mounted in the UHV experimental system and the system pumped and baked.

The purpose of the preparation of the partially M-coated cathode was to enable comparison of M-type and B-type cathode surfaces on the same cathode button. By this means, ambiguities arising from variations in impregnant, underlying matrix structure, processing, temperature, etc., which exist between different cathodes could be completely eliminated, and any differences observed in a side by side comparison of the M-coated and uncoated regions of the surface could be confidently regarded as a function of the coating itself and not due to other factors.

Auger elemental analysis of the surface was then carried out with high spatial resolution, the surface first being imaged in SEM mode with approximately 2000 Å resolution to determine the positions of pore mouths, matrix grains and other surface features of interest.

Prior to cathode activation the M-type osmium coated surface showed only osmium and ruthenium in the flat areas between pores. Barium and oxygen could only be detected by probing with the electron beam directly down a pore. Conversely, the uncoated tungsten B-type surface showed strong barium, oxygen and carbon signals widely distributed across the surface. Area mapping of Ba, O, Os and W with the instrument locked onto appropriate elemental Auger lines confirmed a strong positive correlation between barium and oxygen and tungsten, and a negative correlation between barium/oxygen and osmium. It is likely that the barium and oxygen on the B-type side were present as barium carbonate formed via atmospheric exposure of impregnant. The wide distribution of impregnant residue on the B-type surface was

probably partly due to the process used to remove the osmium/ruthenium sputtercoat (abrasion with alumina paper), which would tend to smear impregnant material across the tungsten surface. However, an identical process is commonly used as a final mechanical polishing step to improve the surface finish in the manufacture of commercial B-type dispenser cathodes, hence the B-type surface can be regarded as typical.

After activation of the cathode ($1150^{\circ}\text{C}_B < 10^{-8}$ torr) the situation altered drastically. The amount of barium, oxygen and carbon on the B-type surface dropped rapidly until the surface partially stabilized with a thinner layer essentially containing only barium and oxygen. By contrast the osmium coated M-type surface showed increasing amounts of barium and oxygen, finally stabilizing with stronger overall barium and oxygen signals than the B-type side. This is well shown in Figure 6, which comprises a series of Auger line scans across the interface between the M-type and B-type regions of the activated cathode. The scans were made at cathode operating temperature with a small positive bias voltage applied to the sample to suppress the generation of thermionic electrons.

The ordinate shows signal strength for a particular Auger spectral line, and the abscissa shows surface position on a scale of $1'' = 18$ microns. The electron beam was stepped digitally across the surface along a line at right angles to the interface in 1.5 micron increments. At each analysis point the beam was held stationary while signal integration took place.

The position of the interface between the B-type and M-type surfaces can be clearly seen from the abrupt changes in osmium and tungsten signal levels. The expected negative correlation between osmium and tungsten is very marked in the lower two traces of Figure 6 .

Comparison between the two upper traces, showing barium and oxygen, indicates a clear correlation between the two, the oxygen distribution being apparently somewhat more inhomogeneous than that of the barium. The oxygen distribution also correlates with the broad features of the osmium distribution. Further, the total amounts of barium and oxygen are both higher on the osmium-coated side than on the tungsten. Indeed it is

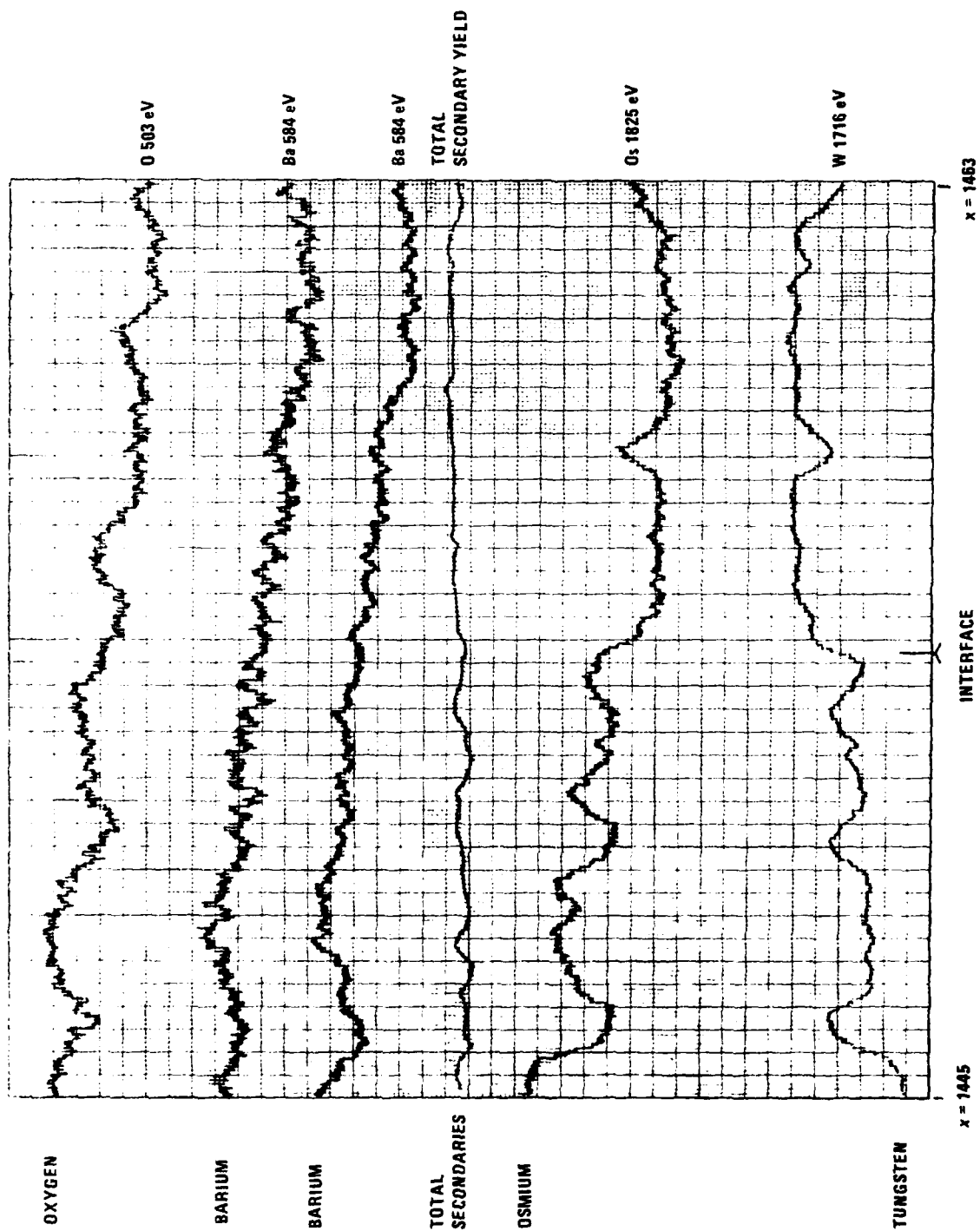


FIGURE 6. SINGLE ELEMENT AUGER LINESCANS ACROSS INTERFACE BETWEEN B-TYPE AND M-TYPE CATHODE SURFACES

possible to draw a horizontal datum line through both the oxygen and the barium traces such that, in each case, the signal level is always higher than the datum line on the M-type side of the interface and always lower than datum on the B-type side.

Comparison of these traces with that for the total secondary electron yield (which can be regarded as a reference signal level) shows no correlation between any of the traces and that for total secondaries. The total secondary yield is slightly higher on the B-type side, but this could be a topographic effect related to average surface roughness. This result does, however, cast serious doubt on the assumption sometimes made by workers in the field that high secondary yield is symptomatic of low work function and therefore may be used as an indicator of thermionic emission capability.

This initial experiment, therefore, showed a clear qualitative difference between the B-type and M-type cathode surfaces when activated, in terms of a greater concentration of both barium and oxygen on the M-type surface. However, the stepped line scan used made no distinction between the contributions from pores and grain tops; in addition, the possibility of surface damage by the stationary electron beam during the signal integration period could not be discounted.

5.2 OTHER CHANGES DURING ACTIVATION

5.2.1 Changes in Osmium/Ruthenium Film

During Auger studies of the M-type portion of the cathode prior to activation it was observed that the osmium/ruthenium film coverage was continuous, very little tungsten signal being observed. However, on the initial heating of the cathode during activation visible (in SEM mode) changes in film morphology occurred, with an apparent increase in film surface roughness. In parallel with this effect tungsten lines appeared in the Auger spectrum of the M-type coated surface thus indicating a change in surface composition from 80:20 Os:Ru to a ternary mixture of approximate composition ratio 35:52:13 W:Os:Ru. This change took place rapidly

(< 1 hour) and the Auger line intensities then stabilized at levels equivalent to the above surface elemental composition with little or no change during further heating.

It was initially felt that alloying by means of interdiffusion between the osmium/ruthenium sputtercoat and the underlying tungsten matrix had taken place; however, consideration of published estimates²⁰ of the probable interdiffusion rates coupled with the relatively low temperature of the cathode surface (1150°C_B max) indicated that such an apparently high degree of alloying would require either a far higher temperature than that employed or, alternatively, a time period several orders of magnitude longer. The step-function nature of the change in observed composition was also inconsistent with any interdiffusion-based process. A far more plausible explanation of the observed abrupt increase in the tungsten Auger signal on initial heating is not alloy formation but rather microcracking of the osmium-ruthenium sputter coat under thermal stress to partially expose the underlying tungsten to the electron beam. Microcracks narrower than 2000 \AA in width would be below the resolution limit of the instrument and hence would not be imaged. Cracks of this order of width or narrower could propagate completely through the sputtered film (only 4000 \AA thick), and their formation on initial heating is completely consistent with the highly stressed nature of sputtered metal films. This explanation would also account for the step function behaviour of the observed change.

5.2.2 Impregnant Residues on the B-type Surface

On the B-type region of the cathode surface the activation process caused an overall reduction of barium carbon and oxygen signals, the oxygen signal was reduced to a greater extent than the barium signal (i.e., the Ba/O ratio increased), and the carbon signal decreased enormously, essentially falling below the noise with normal scan rate and integration time. After activation the majority of the surface was covered by a thin layer of barium and oxygen, sufficiently thin that a strong Auger signal was obtained from the underlying tungsten. In very localized regions, however, the barium oxygen coverage was thick enough to almost obscure even the 1716 eV and 1773 eV at high energy tungsten lines. These "thick-layer regions"

were in many cases not associated with pores. With the cathode at normal operating temperature, a slow reduction in the proportion of B-type surface with "thick-layer" coverage was observed.

It seems likely that the thick-layer regions represent impregnated residues mechanically smeared across the surface during the removal of the sputtercoated film. These regions were (in cathode lifetime terms) a short-term phenomenon and, after 700 hours running, had essentially disappeared. The evaporation and cleanup of such surface residues, which are probably present on the majority of commercial B-type cathodes, may well be a major factor in the stabilization of cathodes which occurs after activation and can take up to 1000 hours depending upon running temperature.

5.3 HIGH RESOLUTION MEASUREMENTS OF EMISSIVE LAYER THICKNESS AND COMPOSITION

Having achieved very promising results with the initial qualitative comparisons of the M-type and B-type regions of the cathode surface, it was decided to attempt to refine these measurements in two directions: First, to work at higher resolution and to discriminate between pores and surface grains and second, to attempt to place the data on an at least semiquantitative basis. At this point the B-type region of the cathode surface had not yet stabilized and during the slow 700 hour cleanup of the surface, the time was utilized to make some necessary preliminary calibration experiments.

5.3.1 Determination of Damage Threshold

Experiments were carried out to investigate the power threshold in the analysis area of the Auger system at which electron beam damage occurred. With a stationary finely focused spot beam damage was seen with a 7.5 kV, 1.5 μ A beam. The threshold power density appeared to be of the order of 1.5×10^5 watts/cm², above which rapid desorption of oxygen from the cathode surface was observed (see Figure 7). In order to avoid this effect, all future measurements were made with the beam rastered over an area of about 10 microns x 10 microns -- the area being chosen by prior

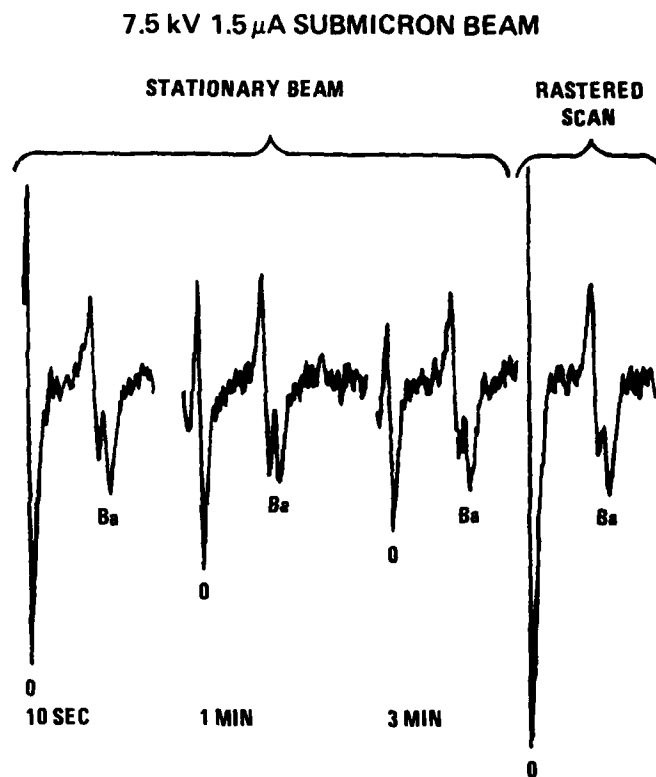


FIGURE 7. LOSS OF OXYGEN DUE TO STIMULATED DESORPTION
DAMAGE WITH STATIONARY BEAM

examination at high resolution to be typical of the type of surface region it was desired to analyze.

5.3.2 Determination of Relative Auger Sensitivity Factors for Osmium and Tungsten

A further necessary preliminary to the next experimental phase was the determination of the relative Auger sensitivity factors for the osmium high energy Auger lines relative to tungsten. This information is not available from the literature except as a theoretical extrapolation²¹.

The measurement required a sample containing areas of pure tungsten and pure osmium with the same surface topography to eliminate secondary emission yield variations arising from surface geometry effects. A suitable sample had been placed on the Auger system carousel at the time of loading the experimental cathodes and comprised a tungsten ribbon, a portion of which had been sputtered with pure osmium (using aluminum foil to temporarily mask the remainder of the surface).

Examination of this sample in SEM mode shows that the osmium surface was much rougher overall than the underlying tungsten. However, at the edges of the masked areas, osmium had penetrated under the foil mask to give a thin feather edge to the film and the very thinnest areas of coating (furthest under the mask) accurately reflected the conformation of the underlying tungsten.

Due to the surface specificity of Auger analysis, even extremely thin films (~ 50 Å) can appear infinitely thick. It was therefore possible to obtain a "pure osmium" spectrum from the extreme edge of the film where the coating was only a few tens of atomic layers thick and to compare this with the "pure tungsten" spectrum from the immediately adjacent uncoated portion of the surface.

The majority of previous workers have used low energy Auger lines as signatures for osmium and tungsten. These present difficulties if used for quantitative analysis, as not only do they occupy a crowded region

of the spectrum but, in many cases, the lines for the two metals are partially superimposed. Only the rather weak 350 eV tungsten line is fully distinct. By far the strongest Auger transitions for the two elements lie in the high energy region above 1500 eV. Tungsten lines at 1716 and 1773 eV and osmium lines at 1825 and 1895 eV are very intense and fully separated from each other (Figure 8).

The main obstacle to the use of these transitions has been the need for a high voltage incident electron beam in order to excite them efficiently and to get good signal to noise without a strongly sloping background. (A typical Auger system electron gun would employ a 3 kV voltage.) When the beam strikes the sample, many electrons are back-scattered to give an extremely intense "elastic peak" at the incident beam energy. This peak has a long tail extending down to lower energies caused by various inelastic processes, and with a low energy incident beam this tail appears in the high energy Auger region as background noise rising very rapidly with energy (Figure 9). The Varian SAM gun will work at up to 10 kV; working at 7.5 kV gives an essentially flat background in the 1500 eV to 2000 eV region of the spectrum. This permitted the use of the high energy elemental lines for analysis with concomitant gains in accuracy.

5.3.3 Quantitative Comparison of B-Type and M-Type Cathode Surfaces

In order to investigate both the thickness and composition of the emissive layer of the mature cathode surfaces, spectra were run comparing the barium and oxygen Auger signals and their strengths relative to the high energy signal(s) from the underlying metal matrix for the dual-surfaced cathode.

Measurements were made at many positions on both B-type and M-type surface regions using a rastered beam confined to the "flat" regions between the pores. This avoided the possibility of errors caused by Auger signals arising from the beam impinging on the impregnant within the pores. Care was taken, by optimizing beam current, signal integration time and

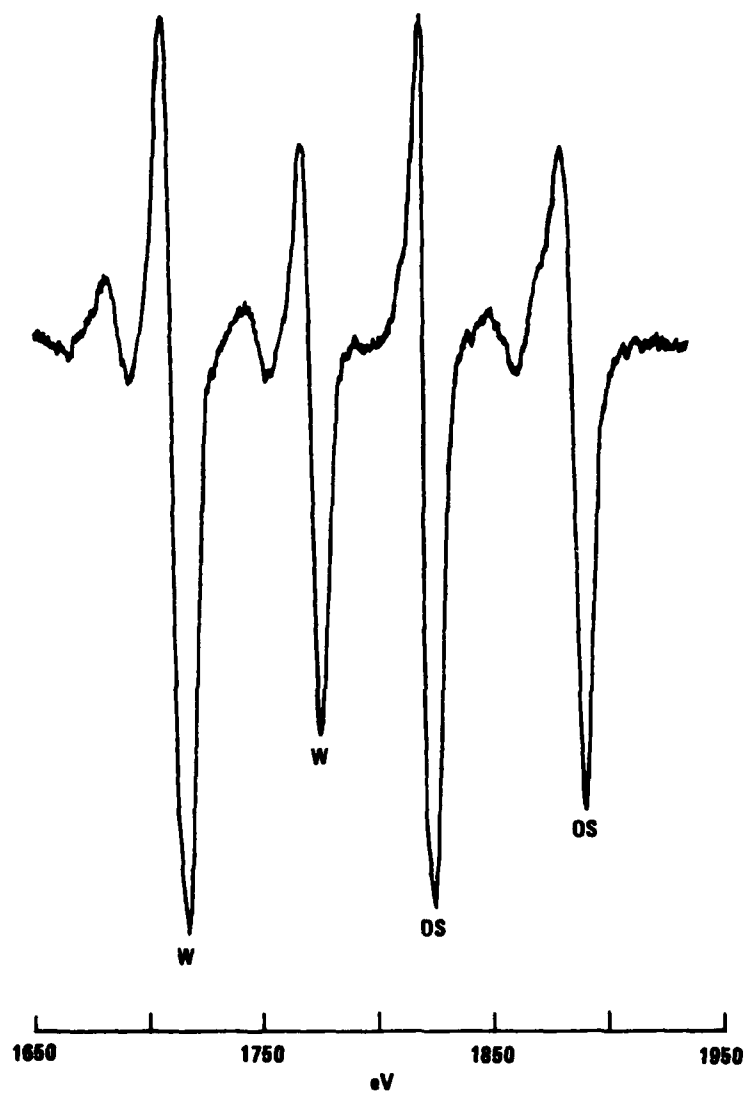


**FIGURE 8. TUNGSTEN AND OSMIUM HIGH ENERGY AUGER LINES
SHOWING SEPARATION AND SIGNAL-TO-NOISE**

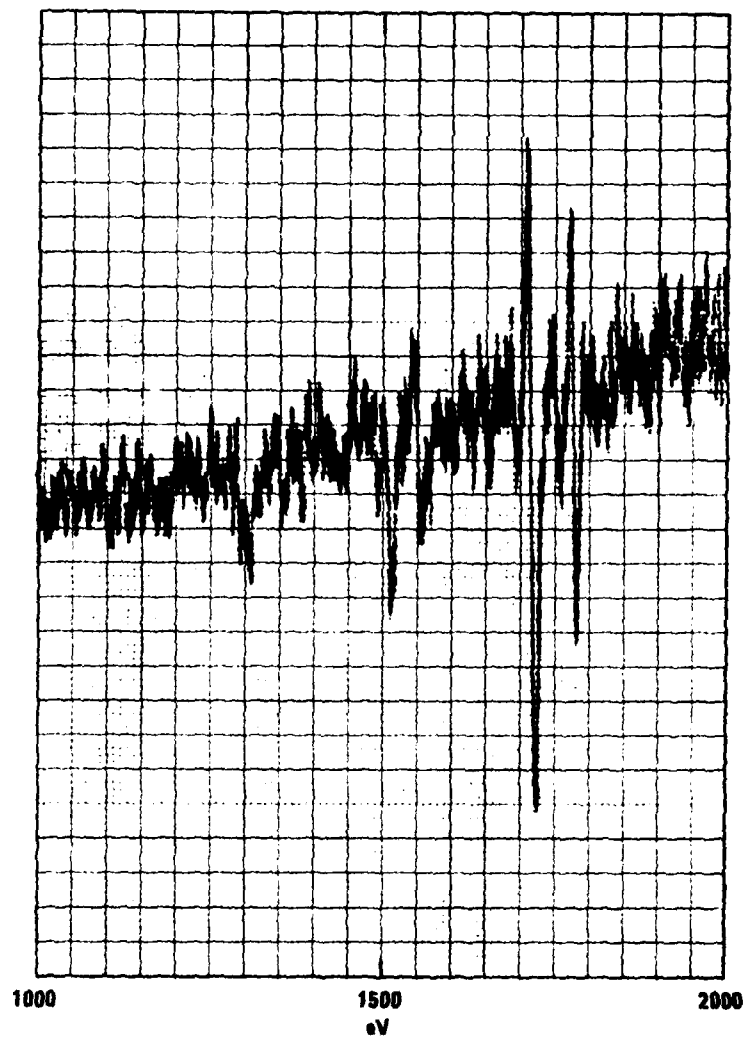


FIGURE 9. AUGER SPECTRUM OF TUNGSTEN SAMPLE HIGH ENERGY REGION WITH 3 keV INCIDENT BEAM

sweep rate, to obtain good signal-to-noise ratio with undistorted peak shapes, thus increasing the accuracy of the peak height measurements (see Figures 10 and 11).

The results obtained were plotted using a method first suggested by Maloney²² which is capable of simultaneously indicating the stoichiometry of the material in the emissive layer and the layer thickness itself.

Initial data for barium oxygen ratios, using the Ba 584 eV and O 503 eV lines showed that the BaO ratio for the interpore regions of the mature cathode surface was remarkably uniform. Intensity measurements of the W 1716 eV and Os 1825 eV lines were also made at coincident points.

Figure 12 shows peak height data from both M-type and B-type surface regions displayed at Ba/W versus O/W. The ratios of the Ba 584 eV peak to the underlying metal signal are plotted on the X axis and the ratios of the O 503 eV peak to the same underlying metal signal on the Y axis. For the purposes of the plot, the Os 1825 eV signal (if present) was converted to "equivalent W 1716 eV signal" using the previously determined relative sensitivity factors. In such a plot, the slope of the line passing from the origin through a point indicates the barium to oxygen ratio at that point. The distance of the point from the origin increases as the relative strength of the underlying metal signal decreases and, since the amount of absorption of the Auger signal from the underlying metal matrix depends upon the degree of barium/oxygen coverage, the distance from the origin is a measure of the emissive layer thickness at that point.

The data plotted in Figure 12 gave very significant results with little scatter. The majority of the points lie almost exactly on a line with a slope characteristic of a Ba_1O_1 stoichiometry. (Bulk BaO gives a peak-to-peak Auger signal strength ratio O 503 eV/Ba 584 eV ≈ 2 .)²³ The only significant difference detected between the B-type and M-type surface regions was in terms of surface coverage. Here, the points fall clearly into two distinct groups with markedly thicker coverage present on the M-type surface.

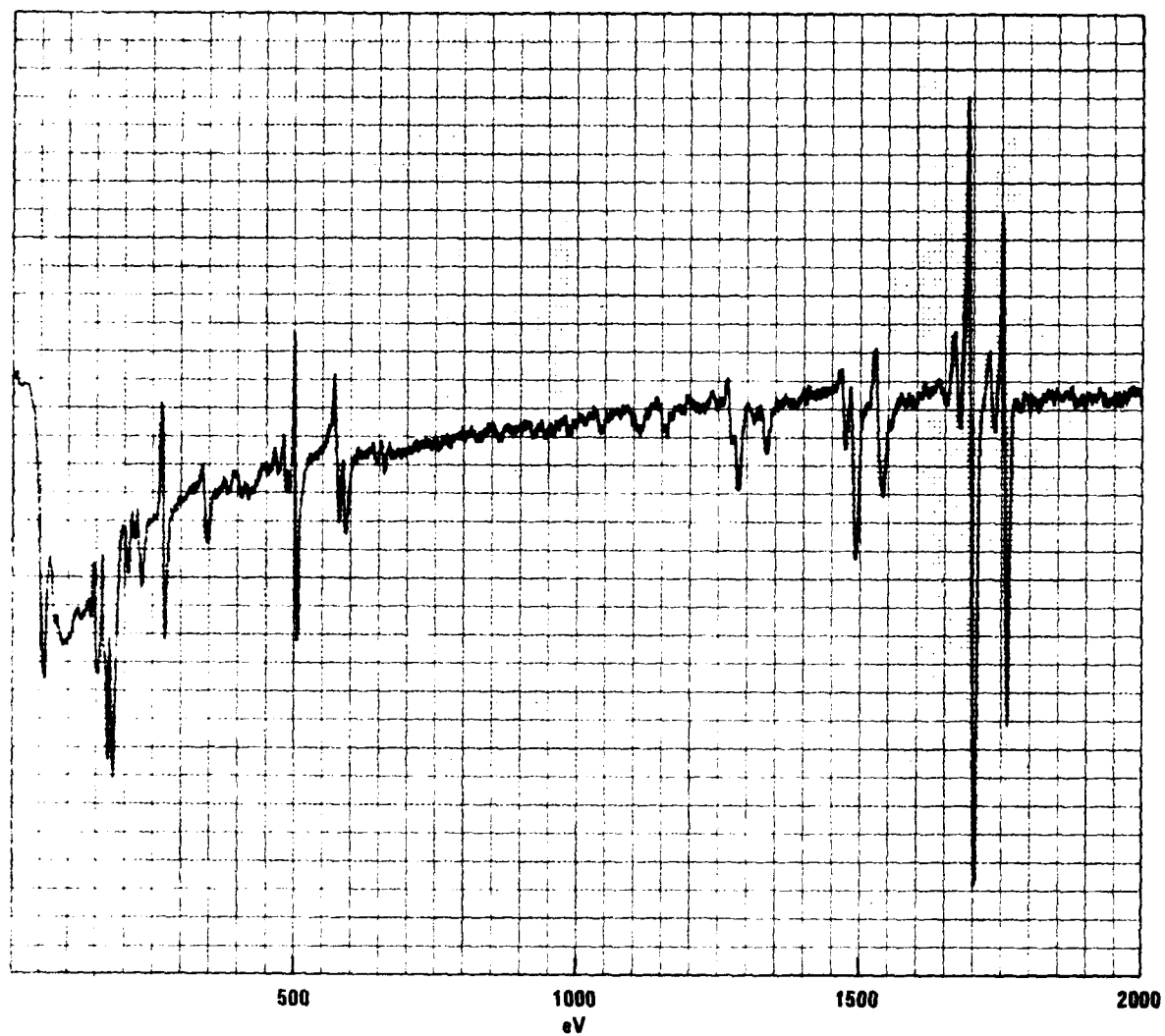


FIGURE 10. FULL WIDTH AUGER SPECTRUM OF ACTIVATED B-TYPE SURFACE (INTERPORE REGION, 1000°C_B)

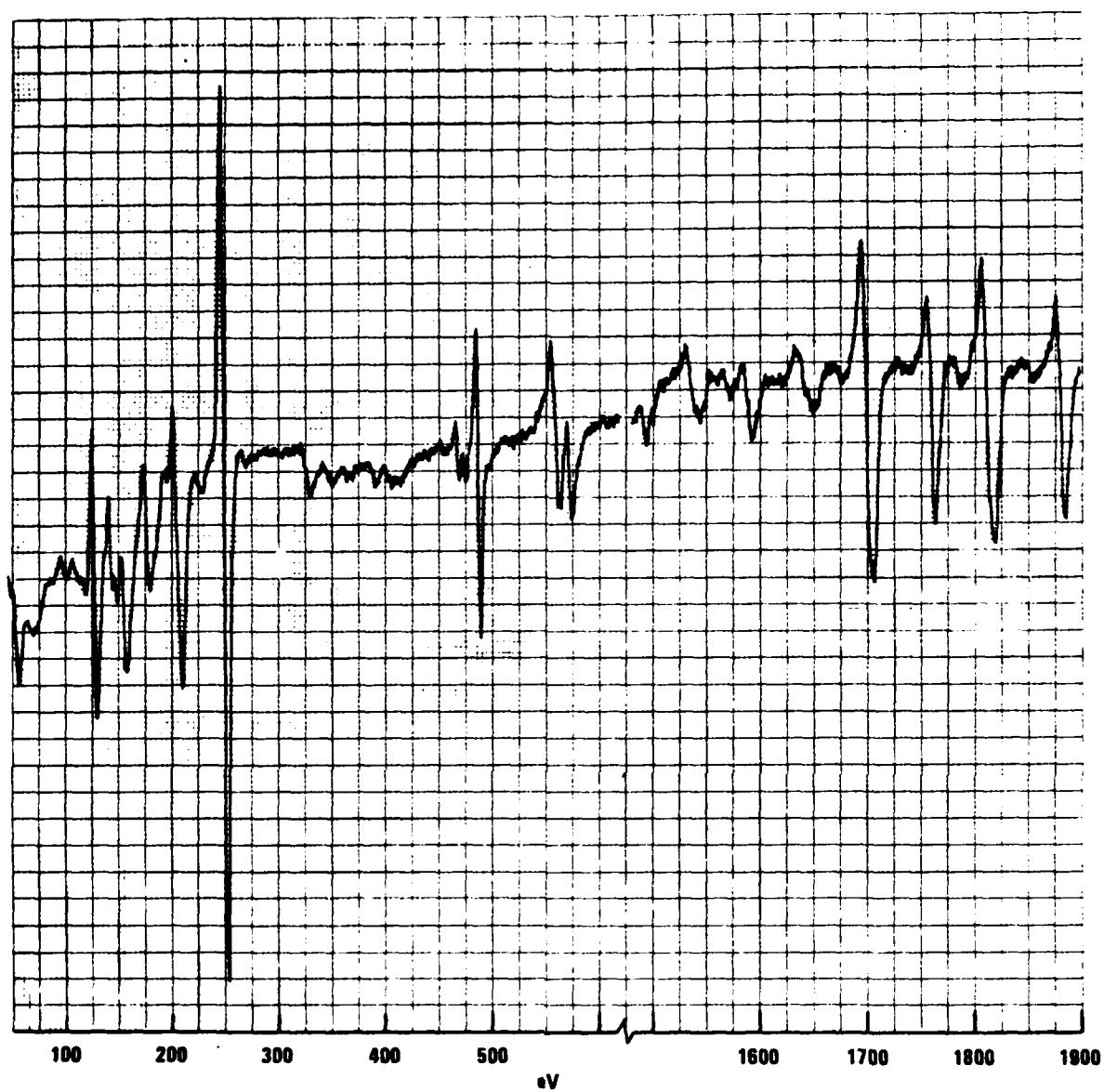


FIGURE 11. AUGER SPECTRUM OF ACTIVATED M-TYPE SURFACE
(INTERPORE REGION, 1000°C_B)

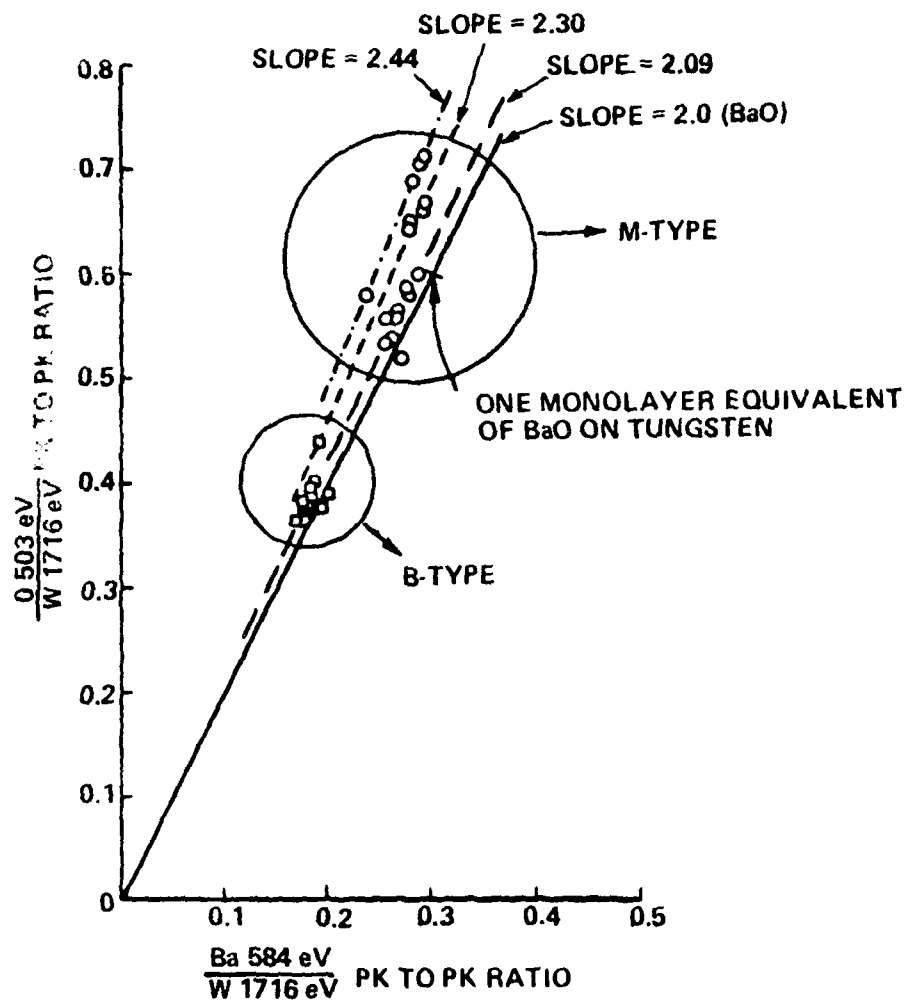


FIGURE 12. PLOT OF O/W AND Ba/W AUGER SIGNAL RATIOS FOR INTERPORE REGIONS OF ACTIVATED B-TYPE AND M-TYPE SURFACES

Thus, the original theory put forward to explain the emission enhancing action of osmium (and certain other platinum group metals), based on their high work functions causing an increased polarization and hence greater surface dipole moment in the emissive layer, is not supported by the Auger data. Instead, the greater emissive capability of the M-type cathode would appear to result primarily from a more stably bound emissive layer and hence a greater average coverage than in the case of the tungsten.

The large amount of oxygen present on the surface is also noteworthy. Early models of the cathode emitting surface in terms of metallic barium on tungsten are inconsistent with the observed data. If the calibration data of Shih, Hor and Haas can be applied to the very thin layer of material present on the surface of the cathode, then there is approximately one oxygen atom for every barium atom present in the emissive layer. Indeed, far from being oxygen deficient with respect to a Ba_1O_1 stoichiometry, the surface between the pores and especially the M-type region has an emissive layer composition which appears to lie on the oxygen-rich side of this ratio.

5.3.4 Absolute Thickness of Emissive Layer

It is difficult to estimate the absolute thickness of the emissive layer because of the possibility of nucleation effects below the resolution limit of the electron beam. Some guidance can be obtained from consideration of the relative signal strengths of the W 169 eV and W 1716 eV Auger lines. The lower energy Auger electrons will be much more strongly absorbed in passing through the emissive layer and therefore, the ratio of the peak-to-peak heights W 1716 eV/W 169 eV should be greater than for bare tungsten. To a first approximation, nucleation (which will result in thicker regions of barium/oxygen coverage separated by regions of uncoated tungsten) will dilute this effect since the component of the signal coming from the uncoated tungsten will undergo no additional differential attenuation of the high and low energy Auger electrons.

For a tungsten surface cleaned by argon ion bombardment, the ratio W 1716 eV/W 169 eV is 1.59:1 (with 7.5 kV incident electron beam).

For the mature B-type cathode surface (700 hours/1000°C_B) this ratio is 3.8:1. Hence, any nucleation of the emissive layer cannot be extreme and, indeed, the indication is rather that the coverage is quite uniform. On this basis, the emissive layer of both the B-type and M-type surfaces is very thin, probably < one monolayer. The B-type surface coverage averages approximately 60% of the M-type surface coverage.

5.4 X-RAY PHOTOELECTRON STUDIES OF CATHODE SURFACES

5.4.1 Introduction

X-ray photoelectron spectroscopy (XPS) provides a surface analytical tool in many ways complementary to Auger microscopy. Due to the difficulties of producing a small focused spot of X-rays, the technique has little or no spatial resolution. However, the photoelectron spectra obtained are simpler than Auger spectra, at least equally surface specific and, most important, show simple linear line shifts dependent upon the effective nuclear charge (i.e., chemical oxidation state of the analyzed element).

The exact state of the chemical combination of the component elements of the cathode emissive layer has been and still is an area of intense debate. Proposed models have at various times ranged from metallic barium on metallic tungsten through barium on oxidized tungsten to barium oxide on tungsten. Previous published XPS reports on B-type cathode surfaces had indicated that the surface of the tungsten matrix, although oxidized prior to activation, was not oxidized in the activated cathode and indeed, any tungsten oxide present was reduced during the activation process. However, the chemical state of the barium, its form of combination with the oxygen, and the nature of the strong bonding to the metal surface are still areas under investigation.

Our own in-house XPS system was not delivered until the end of 1980; and the work described in this section was carried out earlier at an external contract research organization where time on an XPS system could be rented. These circumstances set severe limits on the types of experiments

which could be done, in particular to the length of time for which the cathodes could occupy the system. Nonetheless, it proved possible to load the cathodes, bake the system overnight, and then activate and run for some 24 hours at normal operating temperature before taking the final spectra.

The cathodes studied in the system were M-type but with a sputtercoat of pure osmium rather than 80:20 osmium:ruthenium. One of the purposes of the study was to look for evidence of chemical combination between the surface layer of the osmium and the barium and oxygen of the emissive layer. A separate pure osmium standard was therefore also incorporated in the system. Spectra could be run with the cathodes at operating temperature, and it was possible to vary the angle between the cathode surface and the entrance slit of the spectrometer and thus to vary the take-off angle of the exiting photoelectrons relative to the surface (Figure 13). This technique is useful for examining any variation in composition with depth in the first few atomic layers of the analyzed surface. The differences between the first monolayer and the second plus subsequent atomic layers are particularly emphasized.

The XPS results correlated well with the data derived from Auger spectroscopy. Figure 14 shows the spectrum of the reference osmium sample surface after ion bombardment cleaning and Figure 15 shows the M-type cathode surface prior to activation. This spectrum shows additional lines attributable to barium, carbon, oxygen and a trace of tungsten. The cathode at this stage was not exactly equivalent of the M-type surface studied in the Auger system as, apart from the absence of ruthenium, the cathode had been fired for five minutes at 1200°C in dry hydrogen after sputtercoating in order to improve the coating adhesion. This heating cycle inevitably initiated some of the changes involved in cathode activation, the cathode being subsequently exposed to air enroute to the XPS system.

Figure 16 shows the photoelectron spectrum of the M-type cathode at operating temperature after activation within the XPS system. Relative to Figure 15, the carbon signal has dropped below the noise and the oxygen signal has decreased considerably. Also, tungsten lines are clearly

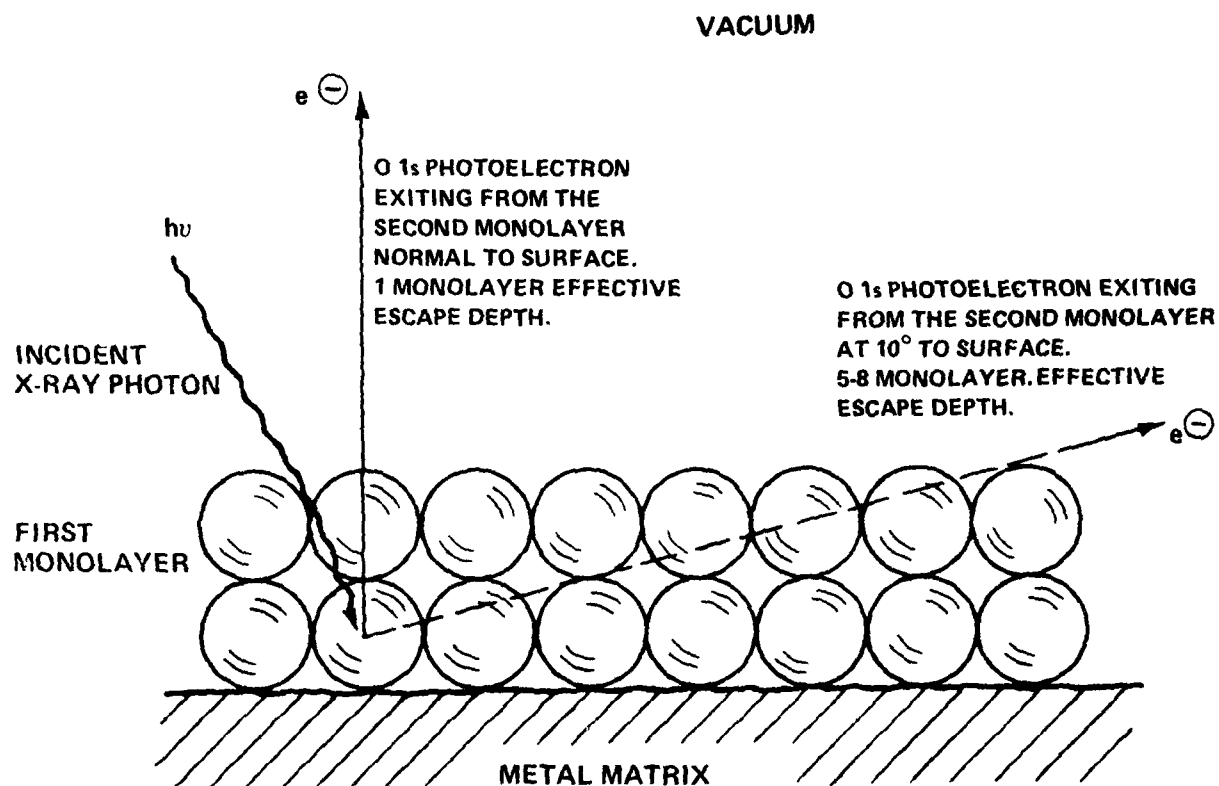


FIGURE 13. VARIATION IN EQUIVALENT ESCAPE DEPTH WITH EXIT ANGLE FOR PHOTOELECTRONS ORIGINATING BELOW THE FIRST MONOLAYER

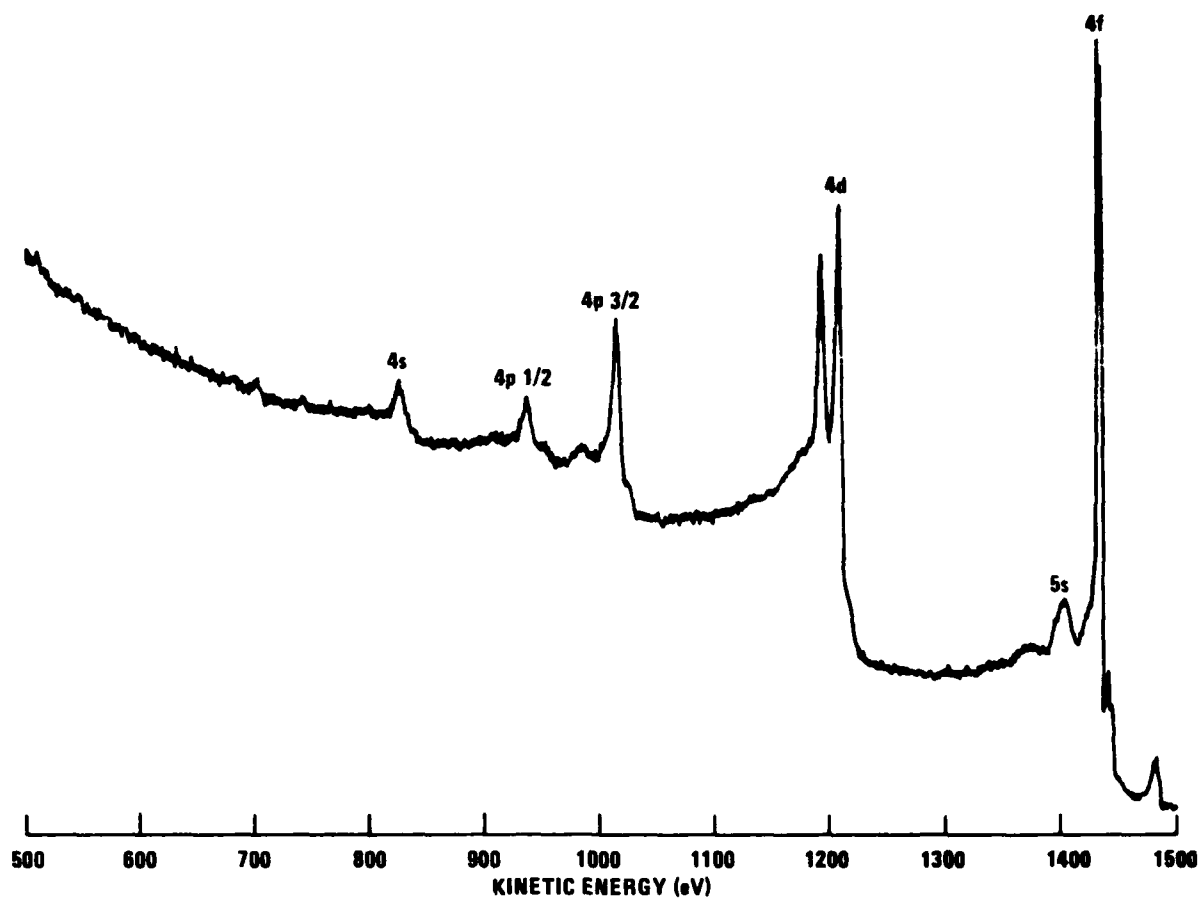


FIGURE 14. X-RAY PHOTOELECTRON SPECTRUM OF CLEAN OSMIUM
REFERENCE SURFACE (ION BOMBARDMENT CLEANED 2X)



FIGURE 15. X-RAY PHOTOELECTRON SPECTRUM OF M-TYPE CATHODE SURFACE PRIOR TO ACTIVATION

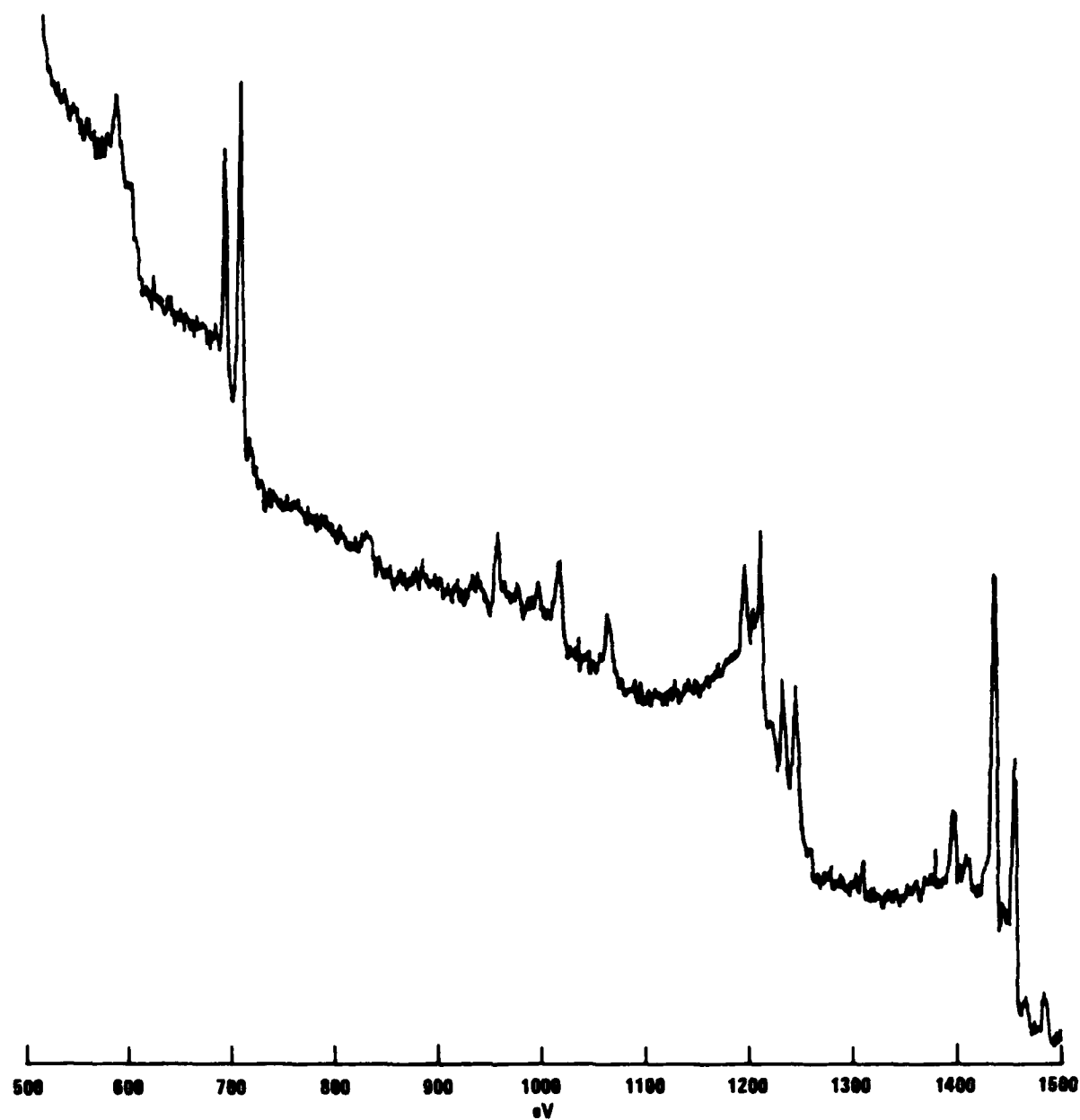


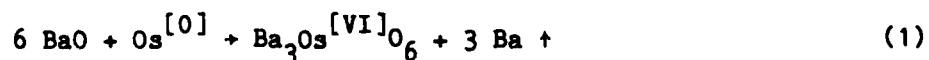
FIGURE 16. X-RAY PHOTOELECTRON SPECTRUM OF ACTIVATED
M-TYPE CATHODE SURFACE (1000°C_B)

visible in the spectrum such that the osmium sputtercoat now appears to contain ~ 30-40% tungsten.

The arguments advanced in the discussion of the Auger data, which also showed a sharp increase in tungsten signal on activation, apply with equal validity here. Cracking of the osmium film on a microscale during the activation heating cycle exposing the underlying tungsten to the incident X-rays seems a more plausible explanation than alloy formation by interdiffusion in view of the time and temperature involved.

The changes in the carbon and oxygen signals can similarly be correlated with thermal decomposition of barium carbonate and loss of CO₂, the carbonate having been formed during the exposure of the cathode to atmosphere in the process of transfer to the XPS system.

The osmium 4f 5/2 and 4f 7/2 doublet was examined at high resolution. The peaks were compared with the analogous peaks of the reference sample, which was electrically at the same potential as the cathode, and no shift to higher binding energy was observed. Such a shift would occur if the oxidation state of the osmium was increased by chemical combination with the barium and oxygen of the emissive layer to form an osmate compound. Such reactions have been reported²⁴ between barium oxide and finely divided osmium in an oxidizing environment, and it was thought that this type of reaction



might explain the stronger binding of the barium and oxygen at the M-type surface and also the apparent high oxygen content of the emissive layer. These compounds which have the perovskite structure are known to have low work functions.

In fact the osmium 4f signal from the activated cathode surface was, if anything, shifted slightly to lower binding energy. This apparent shift could well be an artefact arising from a reduction in analyzer work function due to contamination with evaporant from the cathode. However,

this effect (if real) would imply a transfer of electron density to the osmium rather than the expected reduced screening of the nuclear charge resulting from the oxidative formation of compounds of the osmate type.

Finally, the relative signal strengths of the oxygen 1s line and the barium 3d doublet were investigated at two different photoelectron take-off angles (Figure 17). The barium lines chosen have the same order of kinetic energies (690 and 705 eV) as the oxygen 1s (955 eV) with the exciting radiation used, thus giving similar electron escape depths from the sample.

With a photoelectron take-off angle of 45° to the sample surface, the relative countrate integrals of the high energy barium peak to the oxygen peak were 61:23, a ratio of 2.67:1. However, using a photoelectron take-off angle of only 10° to the surface, the peak area ratio increased to 4:1.

At such shallow exit angles for photoelectrons, the signal from the first monolayer is emphasized, since the effective escape depths for photoelectrons from the second and deeper atomic layers are greatly increased. This effect is of course diluted by any surface roughness or surface curvature which causes variations in the photoelectron exit angle across the sample.

The change in the relative barium/oxygen signal strengths with photoelectron exit angle can only be explained by vertical ordering of the emissive layer. The barium must be concentrated in the top monolayer while the oxygen is below it. This direct measurement, made on an actual cathode at operating temperature, is in accordance with a dipolar mechanism of work function reduction and with the general type of structure predicted previously by Foreman²⁵ from work on model systems and by Rittner²⁶ from considerations of the emissive layer desorption rate.

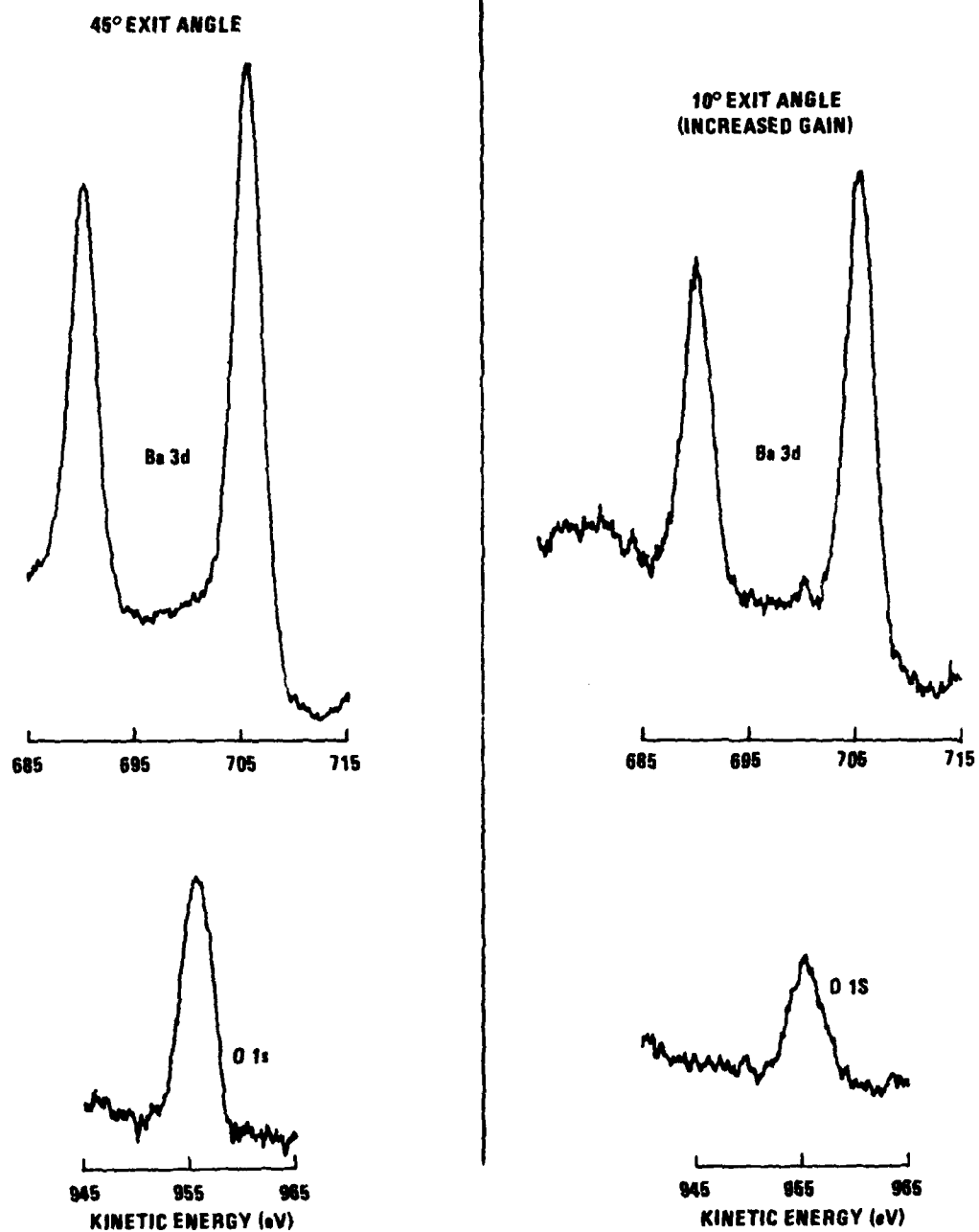


FIGURE 17. VARIATION IN BARIUM AND OXYGEN PHOTOELECTRON COUNT-RATE RATIO AT 45° AND 10° SURFACE EXIT ANGLE FOR ACTIVATED M-TYPE SURFACE AT 1000°C_B

6. A PROPOSED NEW MODEL FOR THE EMISSIVE LAYER STRUCTURE AND
BONDING IN DISPENSER CATHODES AND FOR THE EMISSION ENHANCEMENT
MECHANISM IN "M-TYPE" AND RELATED HIGH CURRENT DENSITY CATHODES

Hitherto in the area of cathode studies, not enough information has been available to permit any definitive description of the nature of the bonding between the components of the emissive layer and of the interaction between the emissive layer and the underlying metal substrate. The present probable consensus among those workers in the field who favor the thin layer model is an almost deliberately broad description of "barium upon oxygen upon tungsten", with the interaction between these components still a matter for experiment and conjecture.

One of the tasks of this research contract was to attempt to construct an improved theoretical model of the physics and structure of the emitting regions of dispenser cathodes. This model must obviously be consistent both with the experimental results obtained during the current research program and with the published data of other workers.

At this point in time, any such theoretical description must be regarded as highly speculative in nature and therefore subject to modification or even complete revision in the light of future experimental data. The remainder of this section should be read with this in mind. Nonetheless, it has proved possible to construct a new, and hopefully improved, description of the structure and bonding of the cathode emitting layer and explain theoretically a number of hitherto puzzling observations including, for example, the mechanism of emission enhancement by the platinum group metals.

The current state of experimental knowledge of the emissive layer structure of dispenser cathodes may be summarized as follows: Auger measurements made on the present contract indicate that the emissive layer consists of a thin layer (of monolayer or submonolayer thickness) of barium and oxygen with a near one-to-one chemical stoichiometry; M-type surfaces show a greater coverage of barium and oxygen relative to B-type surfaces. XPS measurements on M-type cathodes indicate that the emissive layer is

vertically structured with barium concentrated in the first monolayer and oxygen situated below this. The chemical shift data on the osmium 4f peaks show that in the activated M-type cathode the osmium surface is not oxidized but that, if anything, a slight transfer of electron density to osmium has occurred.

Among direct measurements made by other workers, Baun has made an ISS study of B-type cathode surfaces which shows that here too, the top monolayer is highly barium-enriched.²⁷ Jones and co-workers have shown by XPS that the tungsten of a B-type cathode surface is not oxidized when the cathode is activated.²⁸

The oxidation state of the barium in the emissive layer is still a vexed question. Our own measurements on an M-type surface only 24 hours into life show two oxidation states of barium present; this correlates with the data of Jones. However, subsequent to activation, large quantities of neutral metallic barium evaporate from the pores and thus the XPS results quoted may only be relevant to very early life. A more comprehensive study of the barium XPS peaks of activated cathodes has been carried out by a group at Air Force Materials Laboratory²⁹ in which the Ba MNN Auger transition was used as an internal reference and its energy separation from the Ba 3d 5/2 XPS peak measured. Measurements by these workers on more mature B-type cathodes at operating temperature showed an apparent barium oxidation state midway between that of bulk BaO and that of metallic barium on tungsten.

Our own high spatial resolution Auger measurements indicate that the chemical state of the oxygen of the emissive layer on the grain tops is different from that of the oxygen within the pores early in cathode life. The measurements were made at 1050°C_B, at which temperature the pore contents should be conductive enough to prevent the observed small shift of the 0 503 eV line being caused by charging effects.

This Auger line shift presumably represents the difference between the chemical environment of the oxygen in the bulk oxide crystal lattice of the solid masses of impregnant residue initially present in the pores and the

monolayer or submonolayer situation in the emissive layer proper. The rather sparse Auger spectrum of oxygen precludes any more detailed conclusions about the actual chemical state of combination of the oxygen in the emissive layer. However, the low energy barium Auger spectrum of the activated cathode surface, although clearly different from both that of a barium metal monolayer on tungsten and that of barium oxide on tungsten, contains transitions which can be assigned by reference to the Mg/O, MgO low energy Auger³⁰ as characteristic of barium bound to oxygen in an oxide-like situation.

So, to sum up, the following observations must be accounted for.

- 1) The emissive layer of both M-type and B-type cathodes appears to consist of a barium/oxygen monolayer vertically ordered with barium above oxygen, i.e., a Ba-O-M sandwich structure where M is the metal of the underlying matrix.
- 2) The barium oxygen stoichiometry is so close to 1:1 in the stabilized cathode surface as to suggest that each barium is chemically combined with one oxygen.
- 3) The oxidation state of barium is not that of the free metal, but is intermediate between this state and that of barium in bulk BaO.
- 4) The chemical environment of the oxygen is different from that of oxygen in the bulk crystalline mixed oxide of the impregnant.
- 5) The substrate metal of the matrix or the sputtercoat is not oxidized. During the activation process, any oxide previously present is reduced and the activated surface-substrate is metallic. There are indications that, if anything, electron density has been transferred to the metal.
- 6) The emission enhancement exhibited by M-type cathodes relative to B-type cathodes appears to result from increased barium/oxygen surface coverage arising from some difference in the bonding between the emissive

layer and the platinum group metal relative to tungsten. (As a corollary to this, the degree of emission enhancement does not relate to the work function of the underlying metal substrate, either when comparing different metals or different crystal planes of the same metal.)¹⁹

6.1 THEORETICAL MODEL

Two approaches were made to the theoretical analysis of the emissive layer structure.

(1) A study of the type of bonding possible between barium and oxygen in an isolated barium-oxygen moiety, and the nature of the difference between this and the bonding situation in normal barium oxide which is dominated by its ionic lattice.

(2) A consideration of the factors controlling chemisorption on the metals commonly considered suitable for dispenser cathode use, and the interaction of the metal electron orbitals primarily responsible for surface bonding with the above barium-oxygen moiety.

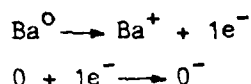
6.1.1 Bonding Between Barium and Oxygen in the Emissive Layer

It is clear, merely from consideration of the mean lifetime of the barium of the cathode emissive layer at operating temperature compared to that of a monolayer of metallic barium on tungsten under similar conditions, that there must be strong bonding between the barium and oxygen of the Ba-O-metal sandwich structure. XPS and Auger data also point to a state of chemical combination between these elements but with marked differences from that existing in normal barium oxide. The XPS data of Lampert²⁹ et al. indicate a barium oxidation state intermediate between that of the metal and the bulk oxide.

Barium oxide is an ionic compound consisting of Ba^{++} ions and O^{--} ions arranged in a closely packed array, bound together by strong omnidirectional electrostatic forces generated by the separated charges. The packing configuration adopted by the ions is that which occupies the

minimum volume and possesses the least electrostatic energy. The driving force for the transfer of electrons from barium to oxygen to give the doubly charged ions is generally stated to be the stabilization energy arising from the formation of the very stable closed shell electronic configurations of these ions. (Ba^{++} is isoelectronic with xenon and O^{--} with neon.) However, this is an oversimplification, as is the picture of this or any other compound as purely ionic.

In practice, the transfer of two electrons from barium to oxygen during the formation of barium oxide requires an input of energy. The transfer of the first electron



is relatively favorable as the first ionization potential of barium is fairly low (5.21 eV), and neutral oxygen has a positive electron affinity for the formation of O^- ion. However, the transfer of a second electron is energetically very unfavorable as the second ionization potential of barium is 10.01 eV and, in addition, the O^- ion has negative electron affinity of 7.3 eV due to the electrostatic repulsion between the single negative charge of the ion and the approaching second electron. The extra energy input necessary for ion formation to occur in fact derives from the enormous lattice energy in the resulting ionic crystal. Barium oxide has the rock salt structure (Figure 18) in which each barium ion is surrounded by six equidistant oxygen ions, while each oxygen ion is similarly surrounded by six equidistant barium ions. In this cubic lattice, if we consider a single positive ion, Ba^{2+} , which has six nearest neighbors (O^{2-} ions) at a distance r , the series of shells of the next nearest neighbors consist of twelve Ba^{2+} ions at a distance $\sqrt{2}r$, eight more distant at $\sqrt{3}r$, six Ba^{2+} ions at $2r$, twenty-four more O^{2-} ions at $\sqrt{5}r$, etc. The electrostatic interaction energy of the Ba^{2+} ions with each of the surrounding ions is equal to the product of the charges on each ion Z^+ and Z^- divided by the distance. Hence, the total electrostatic energy for this barium ion can be written as an infinite series.

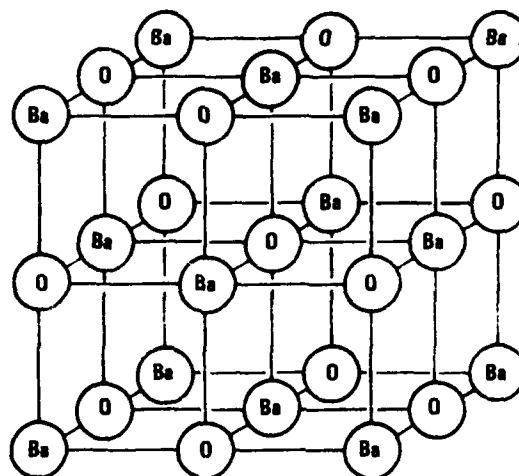


FIGURE 18. THE BARIUM OXIDE CRYSTAL LATTICE STRUCTURE

$$E = \frac{6e^2}{r} (Z^+)(Z^-) + \frac{12e^2}{\sqrt{2}r} (Z^+)^2 + \frac{8e^2}{\sqrt{3}r} (Z^+)(Z^-) + \frac{6e^2}{2r} (Z^+)^2 \dots (2)$$

which reduces to

$$= -\frac{e^2 |Z|^2}{r} \left(6 - \frac{12}{\sqrt{2}} + \frac{8}{\sqrt{3}} - \frac{6}{2} + \frac{24}{\sqrt{5}} \dots \right) \quad (3)$$

The sum of these terms converges to a value 1.747558, the Madelung Constant for the barium oxide lattice structure.

Equation (3) enables an estimate of the electrostatic potential energy of the hypothetical barium oxide lattice with fully doubly charged ions to be made, and this is of the order of 30 eV/ion pair. This is more than sufficient to counterbalance the apparently unfavorable energetics of formation of the Ba^{++} and O^{--} ions and, in addition, to account for the great physical stability of the barium oxide lattice which has, for example, a melting point $> 1900^\circ C$.

In actuality, in even the most ionic compounds, the full theoretical charge transfer does not occur and the bonding between the elements is always partially covalent. However, the properties of crystalline barium oxide show that the ionic component of bonding is completely dominant in this compound.

The mutually bound barium and oxygen of the cathode emissive layer is in an environment very different from an ionic crystal lattice. Here there is only a two-dimensional monolayer sheet of material, and the electrostatic lattice potential energy is essentially non-existent. Because of this, electron transfer from barium to oxygen is much less energetically favorable and the dominant form of bonding between the atoms will be covalent or electron-pair bonding.

Covalent bonding arises when two (or more) atoms are brought into close proximity and the coulomb fields of the atomic nuclei interact with each other and with the atomic electrons in such a manner as to perturb

the wavefunctions characteristic of the electrons in the individual atoms to give new "molecular" electron wave functions of lower total energy. If this occurs, then the configuration with two (or more) closely spaced atoms is stable and a compound molecule results.

In general, the wave equations for the electrons in any polynuclear system are too complex to be solved in an exact and analytical way. Only for certain simpler single atom systems (e.g., the hydrogen atom) are exact solutions available. Hence, approximate approaches have been developed to the problem of describing the covalent bonding in a molecule comprised of an assemblage of individual many-electron atoms.

The exact solutions to the wave equation for the electron of a hydrogen atom are known as "orbitals", and these orbitals may be used as a framework to describe the electronic structure of many-electron atoms. The bonding molecular orbitals formed when atoms are brought closely enough together for compound formation to occur may be described in terms of linear combinations of these atomic orbitals. From the Pauli Exclusion Principle, each atomic orbital (uniquely described by three quantum numbers n , l , and m) can be occupied by a maximum of two electrons which must have opposed spins, specified by a fourth spin quantum number s ($= \pm 1/2$).

In the valence bond approach to combining atomic orbitals, originated by G. N. Lewis and much developed by Linus Pauling³¹, mixing of two individual atomic orbitals is considered to generate two new molecular orbitals, one of lower energy and one of higher energy than the original interacting orbitals. The lower energy molecular orbital is a "bonding" orbital and the higher energy orbital an "antibonding" orbital. Each of these orbitals can accommodate a maximum of two electrons, and an optimum bonding situation is regarded as arising if the interacting atomic orbitals contain a total of two electrons which then completely occupy only the bonding molecular orbital. This is a so-called "electron pair" bond.

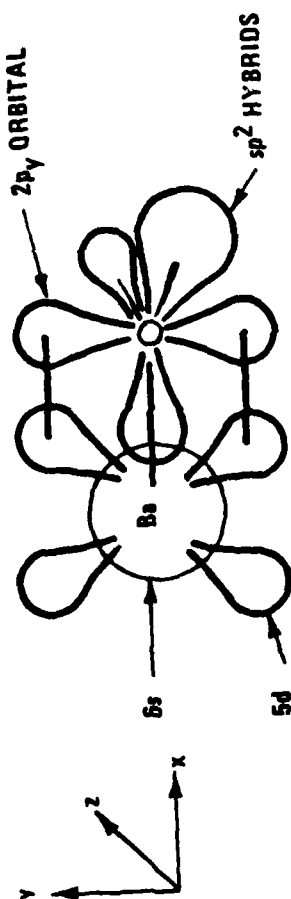
Normally the bonding orbital containing the electron pair is formed from two atomic orbitals, each of which contains a single unpaired electron. However, an electron pair bond can also be formed from the

combination of a filled atomic orbital containing two electrons interacting with a vacant atomic orbital of another atom. In this case, the electron pair is contributed by only one atom and a so-called donor bond results. This involves considerable transfer of charge and is therefore dipolar.

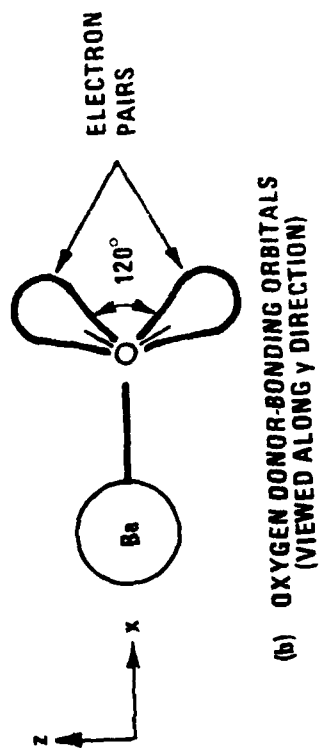
Covalent bonds between identical atoms to give homonuclear molecules involve no net transfer of charge and there is no internuclear dipole or electrostatic component. Nonetheless, extremely strong dipole free bonds can be formed; for example, the purely covalent carbon-carbon bonds in diamond. Heteronuclear molecules formed from atoms of differing electronegatives always possess a dipolar component in the bonding.

In order for two atomic orbitals to interact to form a bonding molecular orbital, three criteria must be met. The orbitals must be of the correct symmetry. They must be of similar energy (i.e., within ~ 2 eV), and finally, they must spatially overlap. This last requirement is almost intuitively obvious and can be physically related to the fact that the more two bonding atomic orbitals overlap, the more the bonding electrons are concentrated between the nuclei, where they can minimize the internuclear repulsion by screening and maximize the attractive forces between themselves and both nuclei jointly. The requirement for good orbital overlap has a tremendous influence on the structure and properties of covalently bound molecules. This arises because all atomic orbitals with 1 quantum number > 0 are not spherically symmetrical. The electron density in an orbital is related to $|\psi|^2$ (the square of the absolute value of the wave function), and plots of $|\psi|^2$ for p, d and f orbitals reveal complex multilobed shapes with the orbital electron density strongly concentrated in particular angular directions. Covalent bonds are thus fundamentally different from ionic bonds in that they are highly directional in character and the interatomic angles in covalently bound molecules or complexes are fixed and constrained to achieve a minimum energy configuration.

Figure 19a shows the orbitals involved in a possible covalent bonding scheme for an isolated barium-oxygen moiety. Two covalent bonds are shown between barium and oxygen, one σ and one π bond, each bonding orbital containing a pair of electrons: one contributed by barium, and one by



(a) BARIUM-OXYGEN BONDING ORBITALS



(b) OXYGEN DONOR-BONDING ORBITALS
(VIEWED ALONG Y DIRECTION)

FIGURE 19. COVALENT BONDING IN "MOLECULAR" BaO

oxygen. This may be compared with the doubly charged ionic bonding between barium and oxygen, which is the situation in the bulk barium-oxide crystal lattice.

The barium ground state configuration is $1s^2 2s^2 2p^6 3s^2 3p^6 4s^2 3d^{10} 4p^6 5s^2 4d^{10} 5p^6 6s^2$, i.e., $[\text{Xe}]6s^2$. Since the 6s orbital energy level is extremely close to that of the 5d (and also the 4f) orbitals, promotion of one electron from the 6s to the 5d level to give a $[\text{Xe}] 6s^1 5d^1$ configuration is energetically feasible, and this gives two unpaired electrons: one in an orbital with σ -bonding symmetry, and one with π -bonding symmetry. Because of the large number of barium orbitals of similar energy to the 6s, this is only one of a number of possible and almost equivalent electronic configurations; all are equally germane to the argument being presented here.

Fortunately, the linking element in the Ba-O-metal sandwich is oxygen, and this "controls" the bonding both to barium and to the metal. In the case of oxygen we have, in toto, only eight electrons to consider. The ground state configuration for oxygen is $1s^2 2s^2 2p_x^2 2p_y^1 2p_z^1$. The 1s electrons are far too low in energy to participate in bonding and may be ignored. This leaves six electrons in potentially bonding orbitals. The oxygen 2s and 2p orbitals are close in energy to the barium 6s and their energy levels are also sufficiently close to each other for mixing of the 2s and 2p orbitals to be feasible. This process generates so-called "hybrid atomic orbitals", and the driving force for hybridization derives from the fact that the physical shapes of the resultant hybrid orbitals are such as to give increased overlap with the bonding atomic orbitals of adjacent atoms and, hence, form a lower total energy combined system. Two hybridization schemes are possible here, sp^2 and sp^3 . Since the end result of both schemes is, in this case, almost equivalent involving only a change in a single bond angle from 120° to 109.5° in going from sp^2 to sp^3 and, further, the real life situation in any case probably involves a mixture of the two hybridizations with sp^2 predominating, only sp^2 hybridization will be discussed.

In sp^2 hybridization, mixing of the oxygen $2s$, $2p_x$ and $2p_z$ orbitals occurs to give three sp^2 hybrid orbitals. These form three lobes of electron density 120° apart in the xz plane (see Figure 20). Each sp^2 orbital can contain a maximum of two spin-paired electrons. The $2p_y$ orbital does not participate in the hybridization and is of slightly higher energy than the sp^2 's. There are a total of six $2s$ and $2p$ electrons to be shared between the four available orbitals, and it is known that the lowest energy configuration is that with the maximum number of unpaired spins. Hence, two of the sp^2 orbitals will have a full complement of two spin-paired electrons each, and the remaining sp^2 hybrid and the $2p_y$ orbital will each contain a single unpaired electron.

The two single-electron oxygen orbitals participate in the covalent electron pair bonding to barium. The sp^2 hybrid orbital on the x axis, which is of σ -bonding symmetry, mixes with the barium $6s$ and each orbital contributes its single electron into a σ -bonding molecular orbital concentrated along the Ba-O axis. Similarly, the oxygen $2p_y$ orbital mixes with a barium $5d$ orbital of approximate π -bonding symmetry and overlap, and forms a (p-d) π -bond. The resultant π -bonding molecular orbital is fully occupied by an electron pair, of which one member is contributed by each of the component atomic orbitals.

Although the two atoms of the barium-oxygen moiety each formally contribute an equal number of electrons to the covalent bonds formed between them, this is not a homonuclear diatomic molecule. The two elements differ greatly in electronegativity and the electron cloud will be localized more about one atom than the other. This gives rise to a considerable dipolar component in the bonding, in this case of form $Ba^{\delta+}-O^{\delta-}$. However, in the absence of the stabilizing influence of a crystal lattice, it will be impossible to support energetically the degree of charge transfer seen in bulk ionic BaO. The bonding in the isolated Ba-O moiety is therefore primarily covalent, with greater shielding of the barium nucleus and reduced effective nuclear charge compared to barium in BaO. This correlates excellently with the Auger and XPS barium spectra which show both highly modified barium-oxygen bonding and a reduced barium chemical shift relative to "bulk" BaO.

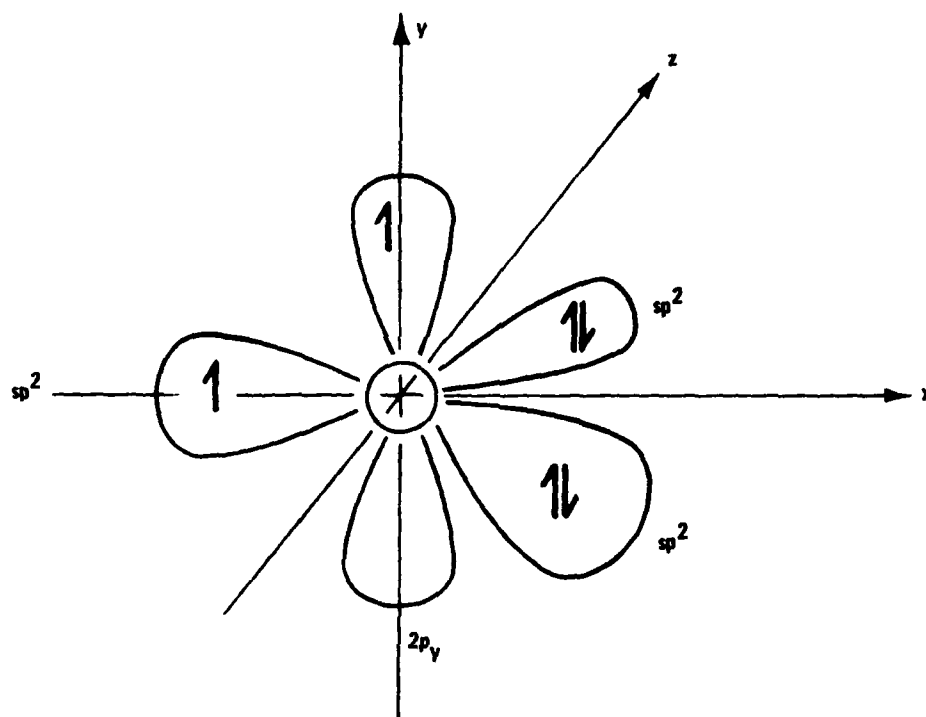


FIGURE 20. sp^2 HYBRIDIZATION OF OXYGEN SHOWING ORBITAL OCCUPANCY

The two remaining oxygen sp^2 hybrid orbitals are both fully occupied, with two spin paired electrons each. They do not participate in bonding to barium. Instead, they protrude in the xz plane to form large lobes of electron density equispaced 120° apart (Figure 19b). These form oxygen "lone pair" orbitals and they are of vital importance in the bonding of the oxygen to the underlying metal surface.

6.1.2 Bonding to Metal Surface d-Orbitals

The valence-bond formalism can also be used to describe the bonding between the covalent barium-oxygen moiety and the underlying metal surface. However, before this is done, it is necessary to digress and to discuss briefly the approach used when considering the metal surface electronic states.

A highly successful theoretical model of the metallic state exists taking into account mainly the experimental results of the study of bulk properties, for example, electrical and thermal conductivities. This model, which considers the properties of delocalized electrons in a constant or periodic lattice potential and takes into account also such parameters as exchange and correlation effects, has been particularly successful in explaining the bulk properties of metals and has also proved useful, although less precise in application, in surface studies. However, the situation where a polyatomic molecule is bound to a metal surface presents a real system so complicated that we are able to describe it only very approximately, and the question arises as to whether the above bulk model is usefully applicable to such questions as the chemical reactivity of a transition metal surface.

One field of study where these questions have been studied in detail is that of catalysis. Tens of billions of dollars of annual industrial chemical production depend on heterogeneous transition metal catalysts. Here, the heart of the process is the binding of molecular species at the transition metal surface.

In investigations of catalytic mechanisms, two approaches exist to describe the interaction of molecules with metal surface atoms. One can either utilize the bulk theory of the metallic state, considering such concepts as the "density of states" at the surface and "holes in the d-band", and treat the interaction therefore as a perturbation of the whole metallic crystal caused by the approaching external molecule; or the surface atoms of the metal can be regarded as reacting more like free atoms toward external molecules, to form a surface complex or "surface molecule", the individual metal atom of which is perturbed by the presence of the rest of the crystal.³² This latter approach has in general proved to be the more fruitful. Much impetus has also been drawn from the recent explosive development of organometallic chemistry where many unusual molecular species are complexed to individual transition metal atoms.

The single atom approach to surface bonding uses, for the electronic structure of the surface atoms, the atomic orbitals characteristic of the individual atom but with fractional occupancy of the atomic orbitals corresponding to the bulk metal value. The model says nothing about the electronic surface states in the absence of a chemisorbed molecule but only makes the assumption that, in the actual interaction between an external atom and the surface of a metal crystal, the wavefunctions describing the states of electrons in the metal surface can be best approximated in the close vicinity of the surface atom by the wavefunctions of an isolated atom of the same metal.

The key orbitals in the surface interactions of transition metals are the d-orbitals. (Surface d-states are known to be highly localized and, in fact, the extent of delocalization of d-electrons within the bulk metal crystal is still the subject of question.³³) In considering covalent bonding to a chemisorbed species, not only the extent of occupancy of the metal d-orbitals is of importance but also the spatial orientation of their emergence from the metal surface. This problem is usually handled by assuming that the direction and type of orbitals emerging into free space is not too different from those involved in formal metal-metal bonds inside the crystal, thus they have directions towards their nearest missing neighbors. Both filled and vacant d-orbitals are of importance in surface bonding, as

the vacant orbitals can also participate in bonding by functioning as electron acceptors.

6.1.3 Classification of Metal Catalysts Based on Surface d-electrons

Transition metals have been classified from the viewpoint of catalysis into four categories or classes according to the orientation and occupancy of d-orbitals extending above the metal surface.³⁴ This classification scheme is highly relevant to the metals normally encountered on dispenser cathode surfaces and to their role in emission enhancement or suppression.

Class I metals (Mo, W) have a vacant d-orbital perpendicular to the metal surface. Class II metals (Rh, Ir, Ru, Os, Tc, Re) have a vacant d-orbital at $36-45^\circ$ to the surface. Class III metals (Fe, Co, Ni, Pd, Pt) have a partially occupied d-orbital at $30-36^\circ$ to the surface. (Class IV metals (Zn, Ga, Cd, In, Ge, Sn, Pb) have not been employed in dispenser cathodes except in poisoning investigations.)

6.1.4 Relative Emission Enhancement Properties of Dispenser Cathode Metal Surfaces

It is now informative to compare the relative emission capabilities of cathodes with various metallic surfaces. Figure 21a shows the arithmetic means (unweighted) of the literature values of emission enhancement obtained for various metals used as surface coatings on dispenser cathodes. The uncoated tungsten dispenser cathode is assigned a reference value of one. For comparison, Figure 21b shows a compilation of the average literature values of the bare work function of these metals. These rise steadily with atomic number and, as previously discussed, show no correlation with the degree of emission enhancement obtained.

Consideration of Figure 21a shows that the metals clearly fall into three categories. Tungsten, the reference emitter, falls into category one. Rhenium, osmium and iridium, the strong emission enhancers, fall into category two. Platinum which, with apparently similar physical properties

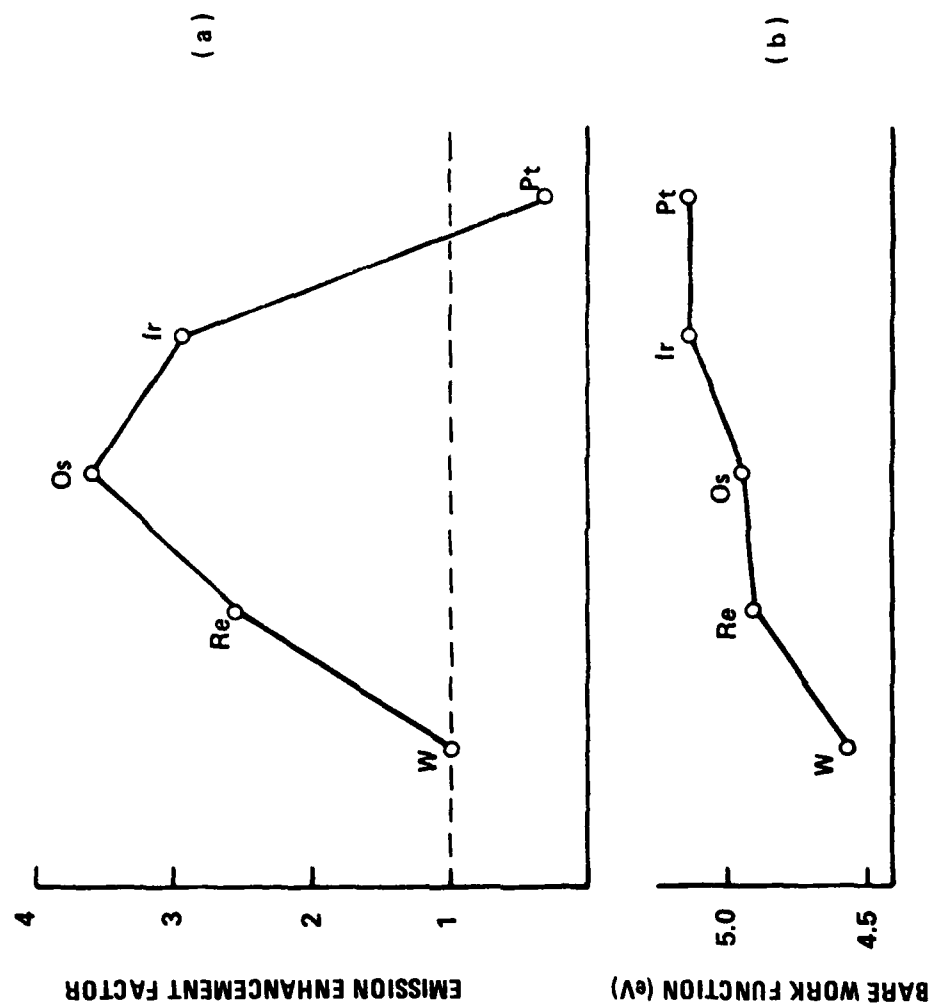


FIGURE 21. AVERAGE EMISSION ENHANCEMENT RATIO vs AVERAGE BARE WORK FUNCTION

and with a very high work function strongly degrades emission, must be placed in a third category. It will be seen that the categorization based on degree of emission enhancement or degradation exactly corresponds to the catalytic classification based on metal surface d-orbitals. Table 1 summarizes this.

Table 1
Comparison of Emission Enhancement with Catalytic
Classification in Terms of Surface
d-Orbitals for Third Row Transition Elements

	Catalytic Classification		
	1	2	3
Standard Substrate	W		
Emission Enhancing		Re, Os, Ir	
Emission Degrading			Pt

6.1.5 Explanation of the Mechanism of Emission Enhancement and Degradation by Metallic Cathode Surface Coatings

The valence bond formalism used to describe the bonding in the barium-oxygen moiety of the emissive monolayer can now be utilized to describe the interaction of the oxygen with the metal surface d-orbitals. Referring to Figure 19a, the oxygen orbitals not involved in bonding to barium and available for bonding to the metal surface are the two sp^2 hybrid

orbitals extending between the x and z axes. However, these orbitals are completely filled and therefore require vacant orbitals into which they can donate their electron pair to form oxygen donor bonds. Further, because of the rigid directionality of covalent bonding, these vacant orbitals must have the correct orientation (for satisfactory overlap) for strong bonding to occur.

Figure 22 illustrates the bonding of the oxygen sp^2 hybrid orbitals of the barium-oxygen moiety to the various categories of metal surface. It can be seen that, in the case of the Class I metal tungsten, only a single vacant d-orbital protrudes normal to the surface, and overlap can therefore occur with only one oxygen sp^2 hybrid, forming a single donor bond. In the Class II metals (rhenium, osmium and iridium) two vacant orbital lobes are available, orientated suitably for overlap with both oxygen sp^2 hybrids. Two donor bonds can thus be formed, giving a stronger total bond. Hence, a higher heat of adsorption should be expected and in a limited supply situation a greater total emissive layer coverage. In the case of the Class III metal platinum, no suitable vacant orbitals exist, only partially filled orbitals which are at best weak electron acceptors. Hence, oxygen donor bonding will not be favored, resulting in weak binding of the emissive layer and reduced surface coverage.

6.1.6 Second-order Effects

Two second-order effects should be considered, which complement the above differences in predicted emissive layer properties.

First, the donor bonds from oxygen to the metal involve transfer of electrons from oxygen to the metal (this is exactly in accordance with the XPS spectra of the activated metal surfaces). The withdrawal of electron density from oxygen enhances the barium-oxygen dipole, $Ba^{\delta+} - O^{\delta-}$, and this effect increases with the amount of donor bonding. Hence the emissive layer dipole may be expected to be greater on the Class II metals.

Second, the directionality of covalent bonding means that, because of the 120° angle between the sp^2 hybrid orbitals, the maximum

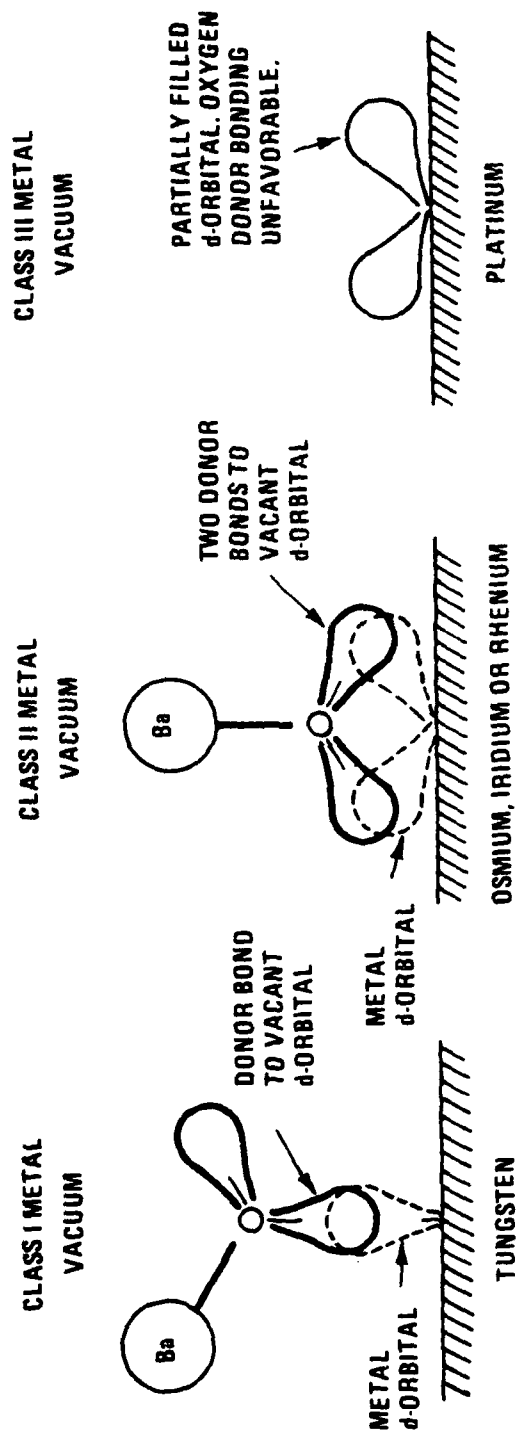


FIGURE 22. COVALENT BONDING TO METAL SURFACE d-ORBITALS

overlap situation for the single donor bond to the Class I tungsten surface is with the barium-oxygen axis at an angle to the metal surface. Hence only a component of the barium-oxygen dipole moment will act in a direction normal to the metal surface to lower the metal surface work function.

This orientation effect may also be one of the factors controlling the work function differences between different crystallographic planes of the same metal. This is because the orbital angles shown in Figure 22 for the various classes of metals are those for preferred crystal planes. Although the number, type and occupancy of the orbitals will remain unchanged, as will the angles between the lobes, the angle of the complete set of orbitals to the surface will vary with crystal plane. Although gross differences between the classes of metals will be preserved, it may be seen that this will affect all aspects of the bonding to the barium oxygen moiety to the metal and, as a result, considerable differences in surface work function should be obtained between individual crystal planes.

6.1.7 Extension of Model to Other Systems

The key feature of the cathode surface metal that determines its suitability as an emissive layer substrate is therefore postulated to be the presence of multilobed vacant surface d-orbitals capable of accepting electron density from the filled oxygen sp^2 hybrids of the barium-oxygen system. It should be noted that the requirement to act as an electron acceptor limits the possible metals to the less electropositive elements at the right hand side of the periodic table transition metal d-block. Strongly electropositive elements to the left of the periodic table, such as zirconium, are disqualified because, although they formally possess unfilled d-orbitals, they will not act as electron acceptors. Instead, a zirconium oxygen interaction would form an oxide-type combination with transfer of electrons from metal to oxygen. In the cathode surface situation this will give a metal-surface to oxygen dipole moment of form $Zr^+ - O^-$, which opposes the barium-oxygen dipole moment and may even destroy the stability of the barium-oxygen linkage.

For good overlap with the oxygen sp^2 "lone pairs", the appropriately angled surface d-orbitals of the metal must protrude adequately from the surface. The third row transition elements have the largest and most spatially extended valence level d-orbitals. This may partially account for differences in performance as emissive layer substrates between the chemically similar second and third row elements in a given group of the periodic table - for example, ruthenium versus osmium, or molybdenum versus tungsten. In the case of the latter pair, it has been reported that a molybdenum surface exposed to the evaporant stream from a dispenser cathode can be activated to the same low work function as similarly exposed tungsten surface, but requires ten times the arrival rate of evaporant as compared to the tungsten³⁵. This would imply a much weaker binding of the emissive layer on molybdenum. One of the factors may be the less favorable overlap resulting from the smaller molybdenum surface d-lobes.

6.1.8 Preferred Crystal Planes

In the work of R.E. Thomas³⁶ on crystal orientation dependence of work function for BaO or Ir, Thomas found that the crystal planes which activated to the lowest work function were atomically rough planes such as Ir(021). Ir(021) is of intermediate bare work function, of the order of 5.3 eV (as compared to Ir(111) at ~ 5.85 eV). Thomas correlated the superior performance of the (021) plane with the observation that the surface of this plane is atomically furrowed, with rows of atoms aligned along the [100] direction. Two studies were cited^{37,38} which indicated, partly from quantum mechanical considerations, that for such atomically rough planes of metal surfaces the surface electron density tends to be concentrated in the furrows rather than the ridges. In this case two very tentative conclusions may be drawn which would suggest that, in terms of the covalent donor bonding model, the ridge atoms might be particularly favorable emissive layer binding sites. One, due to the elevated position of the ridge atoms, their protruding surface d-orbital lobes will be particularly accessible for approach by external interacting atoms or molecules, and good orbital overlap should be achieved. Two, the postulated concentration of electron density in the furrows at the expense of the

ridges should result in a reduced occupancy of the ridge atom d-orbitals, hence rendering them better acceptors for O-donor bonding.

6.1.9 Emission Enhancement in Alloy Systems

Recent advances in the understanding of mixed-metal matrix cathodes indicate that a key factor in the improved emission capability of these devices is the formation of alloys between, for example, iridium and tungsten, which lie in the vicinity of the σ -phase composition. Tuck has investigated the osmium-tungsten σ -phase alloy (a known emission-enhancing substrate superior to pure osmium or iridium) and determined that surface segregation occurs in this alloy at cathode operating temperature.³⁹

Surface segregation is a fairly general property of binary alloys in that the surface monolayer of atoms is composed of only one of the component elements. More usually, but not universally, the surface layer comprises the more volatile of the two elemental alloy constituents. Although the surface atomic layer of the alloy contains only one element, the properties are often highly modified from those of the surface layer of a bulk sample of that pure element.

Tuck has reported results consistent with a surface segregation of tungsten in the first monolayer of the osmium-tungsten σ -phase alloy system. He has observed an oscillatory W-Os-W-Os-structure persisting through the sequence of the first few atomic layers below the surface.³⁹

It is possible to postulate that this structure might improve the emissive layer binding and barium-oxygen dipole moment in the context of the oxygen donor-bonding model. The electronegativities of osmium and tungsten are such as to favor a transfer of electron density from tungsten to the less electropositive osmium. This implies some depletion of electron density from the tungsten of the first monolayer and a resultant slight reduction in the electronic occupancy of the tungsten surface d-orbitals. As already discussed, this will favor O-donor bonding to the alloy surface relative to bulk tungsten; however this factor alone cannot account for the performance improvement of the alloy.

6.1.10 Mode of Synthesis of the Emissive Layer on the Cathode Surface

Although the emissive layer of the cathode surface for a fully activated stabilized cathode appears to have a composition close to a 1:1 barium-oxygen stoichiometry and, in addition, the low energy barium Auger spectrum indicates a barium-oxygen interaction, it would be wrong to refer to the barium-oxygen moiety of the emissive layer Ba-O-metal sandwich structure as "barium oxide". The bonding scheme presented in this discussion requires the linkage to the vacant underlying metal d-orbitals to withdraw electron density from the oxygen lone pair orbitals, which enhances the barium-oxygen dipole and stabilizes the orientation of the barium-oxygen axis such that barium is above oxygen and away from the metal surface. The barium-oxygen moiety probably somewhat resembles, in its internal bonding, a vapor-phase barium oxide "molecule". However, in barium oxide vapor the barium-oxygen ionic charge transfer (and hence dipole moment) must be considerably lower than the situation in the emissive layer with its electron donation to the metal surface. Although the bonding scheme for the barium to oxygen linkage was discussed in isolation from the oxygen to metal bond in Sections 6.1.1 and 6.1.5, this was an artificial separation for the sake of clarity in explanation. The barium-oxygen configuration of the emissive layer is only stable while actually interacting with the metal surface d-orbitals. Refraining from describing the emissive layer composition as "barium oxide" is more than a matter of mere semantics; such fine distinctions have fueled controversy since the early days of cathode research!

In this context it is worth considering whether the emissive layer structure can be formed directly from barium oxide proper, in contact with the cathode surface. There is at present insufficient experimental evidence to offer more than a speculative answer to this question. More work needs to be done in this area. However, chemical intuition would indicate that the proposed O-bonded structure for the emissive layer is strongly suggestive of the transition state that would be formed in the initial attack of barium oxide upon those metals with which it reacts to form perovskite-type compounds; for example, with tungsten to form a barium

tungstate and with osmium to form barium osmate. The former reaction is well known to occur within the pores of dispenser cathodes and the latter reaction, which takes place rapidly under oxidizing conditions²⁴, has also been observed in vacuo⁴⁰ in a model system with osmium at 1000°C in contact with bulk cathode impregnant. On the cathode surface the partial pressure of reagent is almost certainly insufficient to drive the reaction to completion, i.e., to the perovskite compound (that is to barium tungstate in the case of a B-type surface). However, since the surface of a cathode is in a continuous high temperature dynamic equilibrium which cannot be "frozen out" at lower temperature, it may be most accurate to describe the Ba-O-metal sandwich structure as a stabilized reaction intermediate or transition state comprising the first stage of this reaction.

Certainly, thin BaO films of monolayer order of thickness deposited onto cathode metals by vapor deposition at relatively low temperatures do not seem to have the same structure as the cathode emissive layer. G. A. Haas¹⁴ has reported LEED data consistent with an epitaxial growth of BaO on Ir(100) at temperatures below those at which cathodes normally operate. This would imply a first layer with both barium and oxygen in contact with the metal, and Haas interprets his data in accordance with this model. For coverages of $\sim 1/2$ monolayer up, annealed at 500°C, he reports the appearance of a "2 x 2" LEED structure in place of the Ir(100) "1 x 1" structure. This represents the 1 x 1 BaO "crystal" structure epitaxied onto the Ir substrate with a lattice angle at 45° to the basic Ir crystal orientation and a lattice constant of 5.46 Å.

If this general type of structure is in fact also applicable to a BaO monolayer deposited upon tungsten, then it is not clear if any true bond between barium and oxygen would remain under such circumstances. The combined heats of adsorption of barium and oxygen as atomic species on tungsten are more than sufficient to compensate for the energy required to break the barium oxygen bond (even that in a bulk ionic lattice). The heat of adsorption for barium on tungsten is, however, considerably less than that for oxygen on tungsten; and at $\sim 1000^\circ\text{C}$, pure barium desorbs from tungsten (versus $\sim 2500^\circ\text{C}$ for oxygen). Thus at typical cathode operating temperatures it might well be energetically favorable for barium oxide,

initially adsorbed with both atoms bound to the metal surface, to undergo a rearrangement reaction to form the Ba-O-metal sandwich structure with only oxygen bound directly to the surface. This rearrangement reaction would be further favored in a dynamic situation where additional supplies of barium and oxygen were reaching the metal surface and would be available to occupy the surface sites vacated by the barium.

Despite the trend of these speculations, however, this author tends to favor as the predominant mechanism in real cathodes an in situ synthesis of the cathode emissive layer from barium and oxygen reaching the surface by different routes - barium, by surface diffusion from the perimeters of the pore mouths, and oxygen, by out-diffusion directly from the bulk metal matrix. Four observations support this hypothesis:

(1) The predominance of barium over barium oxide in the cathode evaporant stream (at normal operating temperature) as measured at Varian by line-of-sight mass spectrometry.

(2) The fact that analyses of the metal of the matrix, even after the high temperature hydrogen firings involved in matrix and bar and cathode button fabrication, show that it contains 4-500 ppm O_2 .

(3) Observations by the author during Auger studies of end-of-life B-type cathodes (5000 hours, $1150^{\circ}C_B$) with detectably increased effective work functions. Here, although both the barium and oxygen signals relative to the underlying tungsten were lower than those reported in Section 5 for fully activated and stabilized cathodes, (thus indicating a general depletion of the emissive layer coverage), the barium signal was relatively much more reduced than that of the oxygen. This is consistent with a fairly full surface coverage of sorbed oxygen remaining at end of life but a very incomplete coverage of barium above it. This is most easily explained in terms of two separate supply mechanisms for barium and for oxygen reaching the surface, barium being the more mobile and less strongly bound species.

(4) Preliminary Auger studies of the re-activation of clean cathode surfaces show that rates of increase of the barium and oxygen Auger signals are initially independent of each other.

However, at this stage, no really firm conclusions can be drawn on the basis of the available data. More experimental work is needed in these areas.

7. SUMMARY AND CONCLUSIONS

Studies of the emissive layers of activated and stabilized B-type and M-type cathode surfaces at operating temperature were carried out using high spatial resolution Auger spectroscopy and X-ray photoelectron spectroscopy.

Spectra obtained from both types of surfaces were consistent with an activating layer consisting of a monolayer or submonolayer film of barium and oxygen. The surface coverage between the pores was uniform and that of the B-type surface was about 60% of the M-type surface value. The composition of the emissive layer was approximately 1:1 barium to oxygen, with slight oxygen enrichment of regions of the M-type surface. XPS measurements carried out on M-type surfaces showed vertical ordering of the emissive layer, with barium concentrated in the top monolayer above the oxygen (a Ba-O-metal sandwich structure). Low energy barium Auger lines were consistent with a barium to oxygen bonding interaction, but of different form from that in bulk barium oxide. Line-of-sight mass spectrometry of activated cathode showed the evaporant stream to be predominantly metallic barium. Auger spectra of end-of-life B-type cathodes showed depletion of the emissive layer coverage. Oxygen coverage was somewhat reduced relative to a cathode at start of life; barium coverage was much more reduced in comparison.

A theoretical model of the bonding of barium and oxygen to each other and to the emissive surface was constructed, consistent with the above experimental data and the published results of other workers in the field. On the basis of known ionization potentials, electron affinities and crystal lattice electrostatic potential energies, a covalently bonded barium oxygen linkage was postulated. The interaction of this covalent barium-oxygen moiety with transition metal surfaces was considered in terms of O-donor bonding to vacant metal surface d-orbitals. A classification scheme in terms of surface d-orbital occupancy and orientation used in heterogeneous catalysis was applied to the metals normally employed on dispenser cathode surfaces. Consideration of the interaction filled oxygen orbitals with vacant metal surface d-levels enabled the mechanism of emission enhancement by Os, Ir and Re relative to tungsten, and the converse emission degradation

by Pt to be explained. The covalent bonding O-donor model was utilized to account for the reported emission enhancement and preferred binding on crystal planes with atomically rough surfaces and also for emission enhancement on mixed-metal cathodes where alloy surface segregation is observed. Second-order effects resulting from the directional character of covalent bonding, which could affect work function via Ba-O dipole orientation and moment, were analyzed. A distinction was drawn between the chemical state of the emissive layer and that of barium oxide, the barium-oxygen-metal sandwich of the activated layer resembling a stabilized reaction intermediate or transition state.

An in situ reaction mechanism for the formation of the emissive layer in operating cathodes was tentatively preferred pending further experimental evidence, i. e. the barium and oxygen being transported to the emission sites by different routes, by surface and by bulk diffusion respectively.

8. REFERENCES

1. R.G. Pohl and M. Williams, "Electron Emission Processes Bibliography for Super Power Cathode Study" May 1960 RADC TR-60-115.
2. R. Levi, J. Appl. Phys. 24 (1953) 233.
3. H. J. Lemmens, M. J. Jansen and R. Loosjes, Philips Tech. Rev. 11 (1950) 341.
4. R. Levi, J. Appl. Phys., 26 (1955) 639.
5. P. Zalm and A. J. Van Stratum, Philips Tech. Rev. 27 (1966) 69.
6. E.S. Rittner, R.H. Ahlert and W. C. Rutledge, J. Appl. Phys. 28 (1957) 156 - 166.
7. W. C. Rutledge and E.S. Rittner, J. Appl. Phys. 28 (1957) 167 - 173.
8. E. S. Rittner, W. C. Rutledge and R. H. Ahlert, J. Appl. Phys. 25 (1957) 1468.
9. R. W. Springer and T. W. Haas J. Appl. Phys. 45 (1974) 5260.
10. R. Foreman, NASA TND-8295 (1976)
11. R. Foreman, IEEE Transactions on Electron Devices (1977) Vol. Ed 24 No. 1.
12. A. V. Druzhinin, Radio Eng. Electron Phys. 10 (1965) 425.
13. A. H. Beck and H. Ahmed, J. Elect. and Control 14 (1963) 623
14. G. A. Haas, A. Shih and R. E. Thomas, App. Surf. Sci. 1 (1977) 59
15. G. Eng and H.K.A. Kan, "Scanning Auger and Work Function Analyses of Cathodes" presented at Tri Services Cathode Workshop, Rome Air Development Center, April 1980.
16. C. E. Maloney and N. Richardson "Combined Emission Microscope and Auger Studies of Dispenser Cathodes" presented at Tri Services Cathode Workshop, Rome Air Development Center, April 1980.
17. A. Shih, G. A. Haas and J. T. Jensen, Jr., "Rapid Reactivation of Shelf Stored Cathodes" presented at Tri Services Cathode Workshop, Rome Air Development Center, April 1980.
18. M. C. Green, H. B. Skinner and R. A. Tuck "Osmium Tungsten Alloys and Their Relevance to Improved M-type Cathodes" presented at Tri Services Cathode Workshop, Rome Air Development Center, April 1980.
19. R. E. Thomas T. Pankey, J. W. Gibson and G. A. Haas, App. Surf. Sci. 2 (1979) 187.

20. J. M. Houston, "High Work Function Coatings on Barium Dispenser Cathodes" General Electric (USA) Rept 67-C-223 (1967).
21. L. E. Davis, N.C. MacDonald, P. W. Palmberg, G. E. Raich and R. E. Weber "Handbook of Auger Electron Spectroscopy" 2nd Ed., Physical Electronics Industries, Inc., Eden Prairie, MN. (1976).
22. C. E. Maloney, C.R.K. Marrian and G. Wyss, App. Surf. Sci. 2 (1979) 284
23. A. Shih, C. Hor and G. A. Haas, App. Surf. Sci. 2 (1979) 112
24. A. W. Sleight, J. Longo and R. Ward, Inorg. Chem. 1 No. 2 (1962) 245
25. R. Foreman, J. Appl. Phys 47 (1976) 5272
26. E. S. Rittner, J. Appl. Phys 28 (1977) 4344.
27. W. L. Baun, App. Surf. Sci, 4 (1980) 374.
28. D. Jones, D. McNeely and L. W. Swanson, App. Surf. Sci 2 (1979) 232
29. W. V. Lampert, K. D. Rachocki, B. C. Lamartine and T. W. Haas, "Some Aspects of Electron Spectroscopic Investigations of Impregnated Tungsten Dispenser Cathodes" presented at Tri Services Cathode Workshop, Rome Air Development Center, April 1980.
30. A. P. Janssen, R. C. Schoonmaker, A. Chambers and M. Prutton, Surf. Sci, 45 (1974) 45
31. L. Pauling, "The Nature of the Chemical Bond, 3rd ed. Cornell Univ. Press, (1960).
32. Z. Knor, Adv. Catalysis 22 (1972) 51
33. W. A. Harrison, Phys. Rev 181 (1969) 1036
34. O. Johnson, J. Catalysis 28 (1973) 503
35. E. S. Rittner and R. H. Ahlert, J. Appl. Phys. 29 (1958) 61
36. T. Pankey, Jr., and R. E. Thomas, App. Surf. Sci (to be published).
37. J. D. Levine, Surf. Sci. 34 (1973) 90
38. R. Smoluchowski, Phys. Rev 60 (1941) 661
39. H. B. Skinner and L. A. Tuck, Research Report "The Surface Physics and Chemistry of Efficient Thermionic Emitters" AFWAL/AADM Contract F49620-79-C-0026.
40. P. Palluel and A. M. Schroff, "Performance and Life Tests of various Types of Impregnated Cathodes" presented at Tri Services Cathode Workshop, Rome Air Development Center, April 1980.

APPENDIX A

An Electron Optical Investigation of Pore Emission Phenomena in High Current Density Dispenser Cathodes

During in-house high current density emission testing of an experimental IR&D mixed-metal matrix cathode a novel failure mode was observed. This failure mode, upon analysis, appeared to relate to a fundamental aspect of the cathode emission process related to emission from the pores and was of sufficient interest from the viewpoint of cathode physics to trigger a further investigation under the auspices of this RADC program.

The original test data from the cathode were plotted using a normalized current plotting technique originated by G. V. Miram of this company. Miram plots comprise constant voltage curves of current versus temperature. The voltages chosen are related to each other by a factor of 1.59:1 which, by the three halves power law, gives fully space-charge-limited currents increasing from curve to curve by a factor of two. The currents are plotted normalized to 100% J for a given voltage (J being the theoretical fully space-charge-limited current for the voltage in question at T maximum). Thus, in the space-charge-limited region, at high temperatures, all the curves should be superimposed and parallel to the T axis. In practice, a small slope is observed in this region due to imperfect temperature compensation and a resultant slight change in diode perveance due to changing electrode spacing with temperature. The onset of temperature limitation of a given current density is shown by the departure of the curve from this straight-line region.

Figure A-1 shows Miram plots for a standard cathode at 23 and 2500 hours life. The degradation of the cathode performance with life can be seen to take the form of a shift of the normalized current curves to higher temperature (i.e., an increase in overall effective work function). The reduced coverage of the cathode surface and resultant increased patchiness of emission shows up as an increased rounding of the "knees" of the current curves. As expected, this effect is more severe at higher current densities. However, the cathode can still provide the peak current density required; but to do this, must run at a higher temperature.

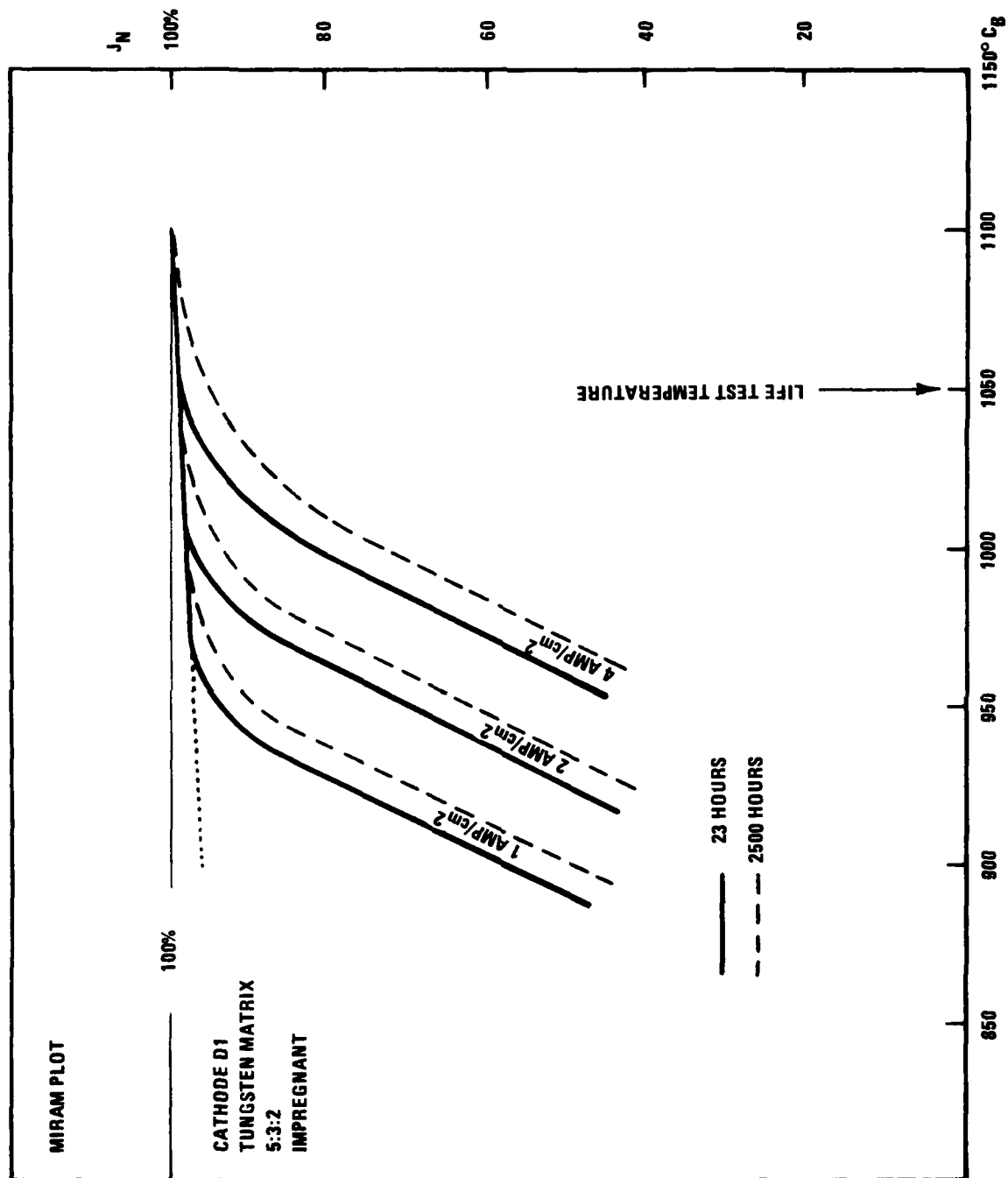


FIGURE A-1. MIRAM PLOT OF STANDARD CATHODE

The high current density mixed-metal matrix cathode, however, showed a completely novel form of degradation of performance with time. Although at lower current densities the behavior was much like that of the standard B-type cathode referred to above, a shift of the normalized current curves to higher temperatures with rather severe rounding of the "knees" being observed, at high current density the phenomena were quite different. Figure A-2 shows the Miram plot for this cathode and the 15 A/cm^2 line shows the full space-charge-limited region with a lower total saturated current. The parallelism of the current line to the temperature axis confirms that in this temperature region the cathode is truly fully space-charge limited. Therefore, a change in perveance (i.e., electrode spacing or cathode area) must have occurred. In contradiction of this, however, the effect is not seen at lower current densities at the same temperature; indeed, the effect is current density dependent. The current temperature curves at lower current densities rule out electrode motion since this effect, being temperature dependent only, would still be seen. Hence, only at high current densities some portion of the cathode surface must become completely non-emitting.

It should be emphasized that this effect cannot be accounted for on the basis of patchiness of work function distribution or upon even the existence of a region of cathode surface completely uncoated with activator and having the work function of bare tungsten. Such a region will emit if the cathode is heated sufficiently, and the increasing emission with temperature would show as slope of the space-charge-limited region of the normalized current curve. Whatever the current density dependent phenomenon is, the affected regions, in emission terms, blank out completely.

The time scale of the performance degradation in terms of cathode operating life, and also certain aspects of the cathode constructional techniques in this case, immediately indicated that the effect could possibly be associated with a reduction in emission at high current densities from the surface pores as their initial filling of impregnant was depleted by evaporation.

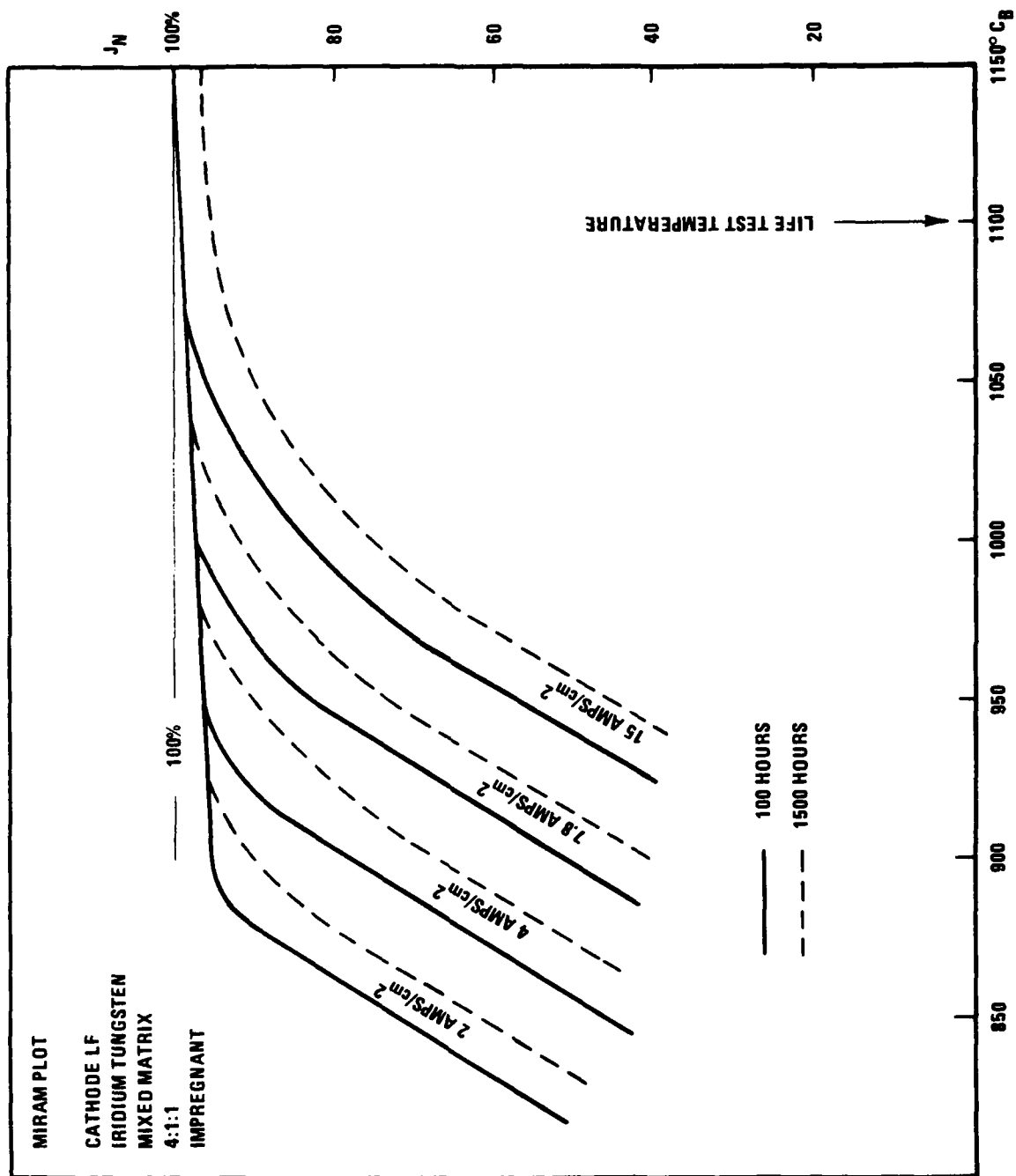


FIGURE A-2. MIRAM PLOT OF MIXED MATRIX CATHODE

Emission from empty pores has always been a question of interest. Since the pores should be lined with a continuation of the cathode emissive surface, they should be filled with a dense space-charge cloud and, at least at low current densities, be good emitters rather like electron analogs of a thermal black body source. However, it seemed possible that at higher current densities the space-charge cloud might become depleted and be unable to support the required rate of withdrawal of charge. This effect would not arise at the beginning of life when the pores would be filled with a solid plug of impregnant which has been shown, by emission microscopy, to be a relatively good bulk emitter.

It was therefore decided to simulate the effect upon the space charge cloud close to the cathode surface of the applied field and the current density drawn, using a Varian proprietary electron optics program. Such programs, in normal use, usually treat emission as arising from a hypothetical uniform sheath of charge. However, they have now reached a state of development where they are capable of handling electron trajectories on a micron resolution scale and within the region between the cathode surface and the potential minimum, where patch fields and space-charge effects completely dominate the applied external field.

Prior to simulating emission from cathode pores, a series of test case studies were carried out in order to gain confidence in the validity of the results obtained. An initial simulation of patch field effects on cathode surfaces was carried out by assigning voltages to annular regions of a planar emitting surface to represent regions of differing work function. Electrons were injected in groups of trajectories with different launching velocities to simulate the half-Maxwellian energy distribution of thermionic electrons. The space charge associated with the trajectories was computed via the line space charge model. The program proved stable under these conditions and the extremely intense fields between "patches" were successfully handled. The effect of increasing the spread of surface work functions (as would occur with reduced supply of emissive material to the cathode surface near end of life) was simulated. Work function spreads of 50, 100 and 150 mV were used. It is known from emission microscopy that

these ranges of work function are not dissimilar to those observed on actual M-type and B-type cathode surfaces.

The requirement to handle the electron trajectories on a micron resolution scale presented no problems for the electron optics program used. However, considerable data preparation effort and analysis plus moderately large amounts of computer time was needed in order to achieve fully converged solutions for each case. In some instances full convergence was not achieved even after many iterations; instead, a damped oscillatory situation was obtained with only asymptotic convergence. Unreasonable amounts of computer time would have been required to obtain further convergence under these circumstances, and the extremes of the solutions obtained were therefore used to set error bar limits around the true solutions.

By varying the voltage of a relatively unperturbed equipotential line outside the potential minimum, about 25 microns from the cathode surface, it was possible to simulate the effect of changing the anode voltage of the diode. Solutions for the total anode current were obtained, and by this means, the current/voltage characteristics of the cathode were simulated. The rounding of the "knee" of the characteristic curve as the work function spread was increased could be clearly seen.

Due to the cylindrical symmetry of the program it was possible to simulate only radial variations in work function. The "patches", therefore, on the model cathode, were of the form of narrow annuli and their perimeter-to-area ratio was much lower than for real "patches" on a dispenser cathode. However, the qualitative agreement between the results obtained in the simulation and the predictions for real cathode was encouraging and gave increased confidence in the validity of the pore emission modeling which was next undertaken.

In this case, an exact simulation of the pore conformation was possible by placing the pore on axis. Current was injected from the cathode surface and from the interior walls of the pore with an approximation to a half Maxwellian energy spread. A uniform surface work function was used. By

varying the equipotential corresponding to the anode voltage, the current density drawn from the surface was adjusted. Figure A-3 shows a trajectory plot for a low current density case and Figure A-4 the high current density situation. It will be seen that, so long as the space-charge cloud above the cathode is not depleted, the pore contributes emission from its internal space-charge cloud as an extension of this sheath. However, when the field penetrates down to the cathode surface, i.e., the potential minimum is less than a pore diameter above the surface, then marked changes are seen. Since the Laplacian field can only penetrate an extremely small distance into the pore which behaves like a hollow cathode^{*}, emission is only drawn from a small region just below the rim. This wall area is not sufficient to support the required emission density across the whole area of the pore and the central region must supply emission from the internal space-charge cloud. The space-charge cloud density already falls off rapidly away from the walls of the pores (due to the energy spread of the thermionically emitted electrons), and the low density central region is immediately depleted. Further supply of electrons from the space-charge cloud deeper in the pore is controlled by drift of electrons driven by the extremely small space-charge potential gradient along the pore, hence the central region saturates.

The current density dependence of the effect is now explained. The effective emitting area of the pore will, in fact, be a function of current drawn due to the space-charge-density gradient from the pore center to the walls. At intermediate current densities, a ring of space charge close to the walls will still be able to support emission, while the central disc or core will have saturated. With increasing current density, the diameter of the saturated disc expands and the width of the emitting annulus shrinks back toward the pore walls. Hence, the effective cathode emitting area is reduced. The key parameter for the onset of this effect is the ratio between pore diameter and the height of the potential minimum above the cathode surface which itself depends upon current density. The need for careful control of pore size in high current density cathodes is thus made clear.

* I. Brodie and A. Niewold, J. Appl. Phys. 33 (1962) 3328

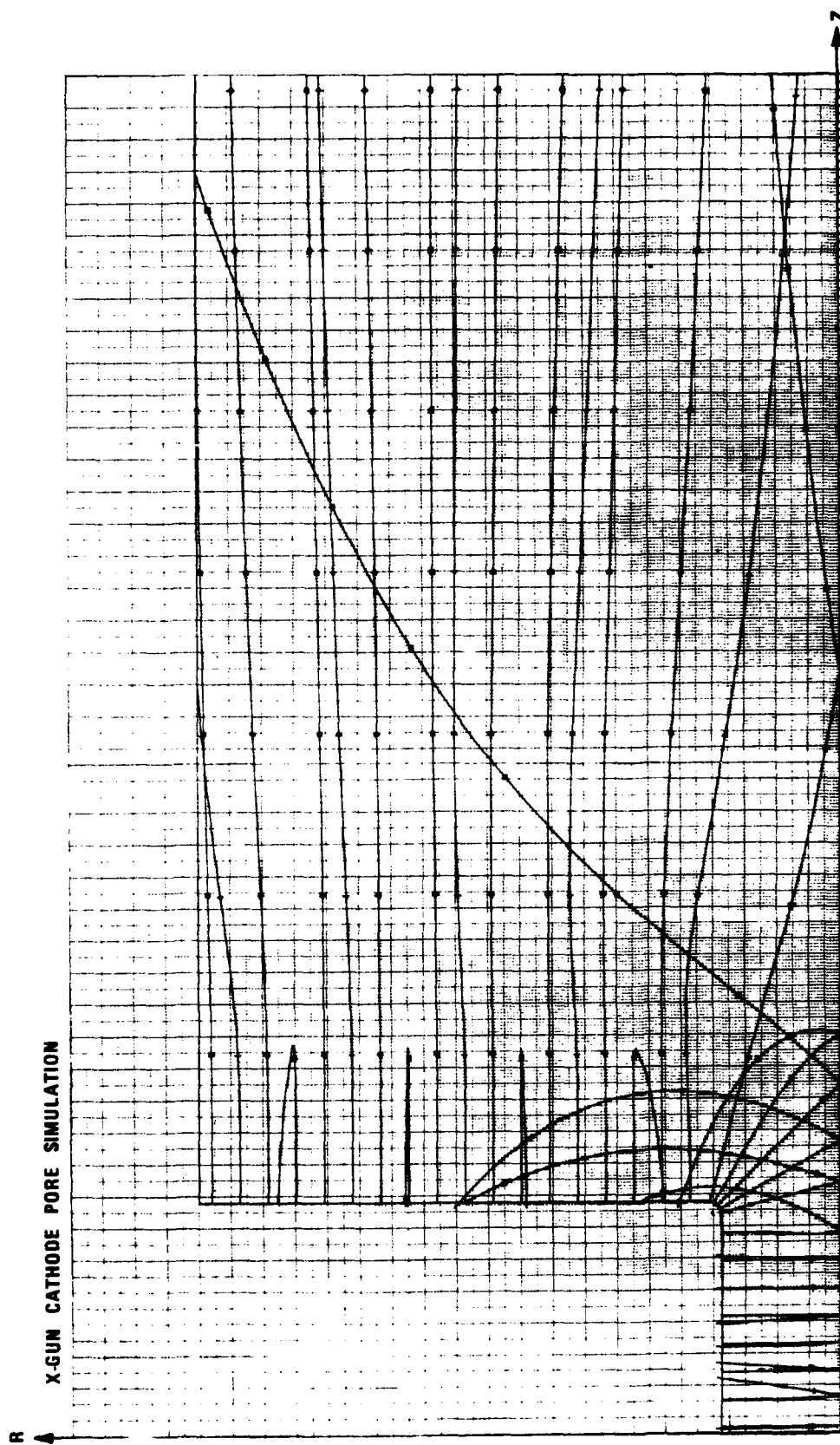


FIGURE A-3. TRAJECTORY PLOT OF PORE SIMULATION AT LOWER CURRENT DENSITY

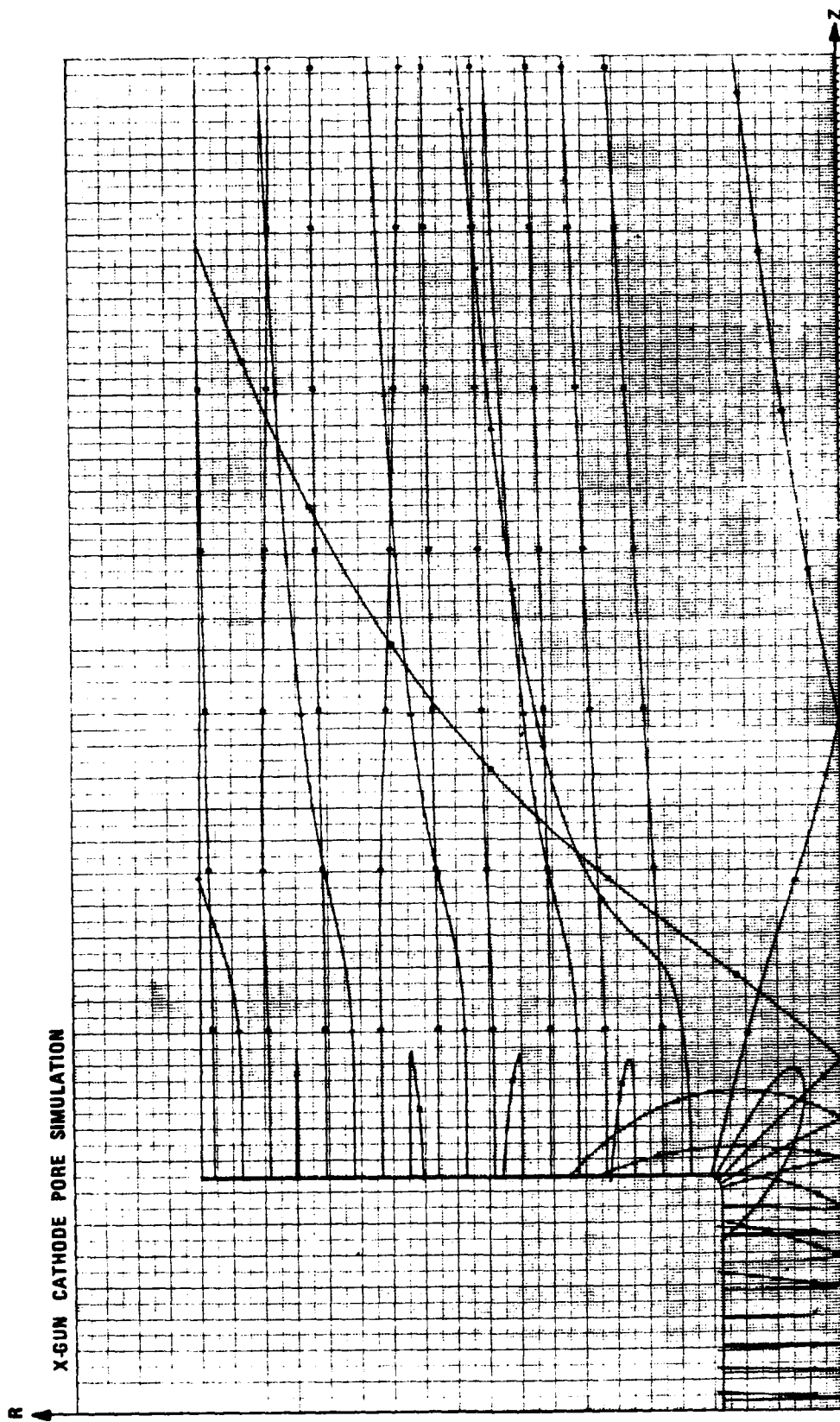


FIGURE A-4. TRAJECTORY PLOT OF PORE SIMULATION AT HIGHER CURRENT DENSITY